Master's Thesis

Biomechanical adaptations in inclined walking

A study of the interaction of the gastrocnemius medialis and the kinematics and kinetics of the ankle, knee, and hip joints

carried out for the purpose of obtaining the degree Diplom-Ingenieurin

submitted at TU Wien

Faculty of Mechanical and Industrial Engineering

by

Lena CASTEL-WOHNLICH

Mat.No.: 11932445

under the supervision of

Univ.Prof. Dipl.-Ing. Dr.sc.nat Philipp Thurner

Institute of Lightweight Design and Structural Biomechanics

Berlin, 05.12.2023

Lena Castel-Wohnlich

I confirm that the printing of this thesis requires the approval of the examination board.

Diplomarbeit

Adaption des humanen Gangmusters bei Steigungen

Eine Studie über die Interaktion des M. gastrocnemius medialis mit der Kinematik und Kinetik von Knöchel-, Knie- und Hüftgelenk

ausgeführt zum Zwecke der Erlangung des akademischen Grades einer Diplom-Ingenieurin

eingereicht an der Technischen Universität Wien

Fakultät für Maschinenwesen und Betriebswissenschaften

von

Lena CASTEL-WOHNLICH

Mat.Nr.: 11932445

unter der Leitung von

Univ.Prof. Dipl.-Ing. Dr.sc.nat Philipp Thurner

Institut für Leichtbau und Struktur-Biomechanik

Berlin, 05.12.2023

[redacted]

Lena Castel-Wohnlich

Ich nehme zur Kenntnis, dass ich zur Drucklegung dieser Arbeit nur mit Bewilligung der Prüfungskommission berechtigt bin.

Eidesstattliche Erklärung

Ich erkläre an Eides statt, dass die vorliegende Arbeit nach den anerkannten Grundsätzen für wissenschaftliche Abhandlungen von mir selbstständig erstellt wurde. Alle verwendeten Hilfsmittel, insbesondere die zugrunde gelegte Literatur, sind in dieser Arbeit genannt und aufgelistet. Die aus den Quellen wörtlich entnommenen Stellen, sind als solche kenntlich gemacht.

Das Thema dieser Arbeit wurde von mir bisher weder im In- noch Ausland einem:r Beurteiler:in zur Begutachtung in irgendeiner Form als Prüfungsarbeit vorgelegt. Diese Arbeit stimmt mit der von den Begutachter:innen beurteilten Arbeit überein.

Ich nehme zur Kenntnis, dass die vorgelegte Arbeit mit geeigneten und dem derzeitigen Stand der Technik entsprechenden Mitteln (Plagiat-Erkennungssoftware) elektronisch-technisch überprüft wird. Dies stellt einerseits sicher, dass bei der Erstellung der vorgelegten Arbeit die hohen Qualitätsvorgaben im Rahmen der geltenden Regeln zur Sicherung guter wissenschaftlicher Praxis „Code of Conduct“ an der TU Wien eingehalten wurden. Zum anderen werden durch einen Abgleich mit anderen studentischen Abschlussarbeiten Verletzungen meines persönlichen Urheberrechts vermieden.

Berlin, 05. Dezember 2023

Lena Castel-Wohnlich

Acknowledgements

I would like to express my sincerest gratitude to Neele Hattermann for her assistance with data acquisition and processing and for her excellent team work. Working and also sometimes despairing with her was one of the most important parts of this thesis.

I additionally would like to especially thank Nicholas Brisson for his exceptional *Visual 3D* pipeline, which was crucial to process the kinematic and kinetic data.

Appreciation is also extended to the members of the *RunScan*-Team at the Julius Wolff Institut (JWI), who gave me the opportunity to ask for guidance during the measurements all the time.

I also want to thank Alison Agres, who supported me with her exceptionally knowledge of the topic and little food for thought when I needed it.

I also want to say thank you, Doris, for keeping me motivated in many situations of struggle. Those times were not easy but you always stayed by my side and withstood several bad tempers.

And thanks to everyone who stopped to ask how my Master's thesis is going!

Abstract

Objective

This thesis describes a study to find interactions and correlations between lower limb joints and muscles during 10° inclined walking with reference to level walking.

Methods

12 healthy subjects performed treadmill walking with a 0° and 10° incline while the motion was captured via a motion capture system, and fascicle length was measured using B-mode ultrasonography.

Results

While eight subjects showed a significant increase in fascicle stretch during inclined walking ($p < .05$) compared to level walking, four did not. Within subjects, fascicle stretch range and maximal dorsiflexion, knee flexion, and hip extension increased by 10° incline compared to 0° ($p < .01$). A correlation was found between initial ankle angle and fascicle stretch range, initial knee angle, and hip extension moment ($p < .05$)

Conclusion

The gastrocnemius muscle is adapted to maintain stability and energy efficiency, varying in length and force application and affecting the joints. In this thesis, the correlation between initial ankle angle and muscle fascicle range of motion were found to change with incline, indicating complex interactions influenced by gait strategies. Although no specific pattern was found in this limited group that could lead to classification, differences in biomechanical gait mechanism were found as a function of inclination.

Kurzfassung

Ziel

Die beschriebene Studie untersucht biomechanische Anpassungen beim Gehen auf einer 10°-Steigung, um Erkenntnisse zur Gehoptimierung zu gewinnen.

Methoden

Die Bewegung 12 gesunder Probanden, die auf einem Laufband liefen, wurden durch ein 3D-Bewegungsanalysesystem aufgenommen. Die Analyse der Faserlänge fand mittels Ultraschalls im B-Modus statt. Alle Ergebnisse wurden zwischen 0° und 10° Steigung verglichen.

Ergebnisse

Bei acht Teilnehmern wurde eine signifikante Muskeldehnung beobachtet ($p < .05$). Neben gesteigerten maximalen Momenten bei Dorsiflexion, Knieflexion und Hüftextension, sowie erhöhten Anfangswinkeln von Sprunggelenk, Knie und Hüfte ($p < .01$), ergaben sich auch Korrelationen zwischen dem initialen Sprunggelenkswinkel und drei weiteren Variablen ($p < .05$).

Schlussfolgerung

Um beim Bergaufgehen eine effizientere Strategie zu nutzen, sollte man den Schritt mit einer höheren Dorsiflexion beginnen. Dadurch wird die Muskeldehnung reduziert und der Muskel kann in seiner optimalen Länge arbeiten. Jedoch beeinflusst diese Anpassung auch die Belastung auf Knie und Hüfte.

Contents

List of Figures xv

List of Tables xix

Abbrevations xxi

1 Introduction 1

2 Background 5

2.1 Biomechanical Aspects of Walking 5

2.1.1 The Gait Cycle 6

2.1.2 Calf Muscle Architecture 7

2.1.3 Biomechanics of the Lower Extremities 11

2.2 Gait Analysis in Biomedical Research 16

2.2.1 Motion Capture 16

2.2.2 Ultrasonography 22

3 Methods 29

3.1 Participants 29

3.2 Experimental Design 30

3.2.1 GRAIL System: Joint Kinematics and Kinetics 31

3.2.2 Ultrasound System: Muscle Architecture 33

3.3 Experimental Protocol 35
3.4 Data Processing 36
3.4.1 Ultrasonography 37
3.4.2 Joint Kinematics and Kinetics 38
3.5 Statistical Analysis 41

4 Results **45**
4.1 Final Sample 45
4.1.1 Excluded Data 46
4.1.2 Participants 47
4.2 Testing Data for Normality 49
4.3 Ultrasound Data 49
4.4 Joint Kinematics and Kinetics 53
4.5 Correlation 59

5 Discussion **63**
5.1 Kinematics and Kinetics of the Joints 64
5.2 Muscular Implications and Contributions 68
5.3 Correlations 70
5.4 Variances Among Participants 73
5.5 Limitations 75

6 Outlook and Conclusion **79**

Bibliography **83**

Appendices **I**

List of Figures

2.1 Physiological human gait cycle[1]. 7

2.2 Physiological muscle interaction during one gait cycle[2]. 8

2.3 Angles of hip (flexion +, extension -), knee (flexion +, hyperextension -) and ankle (dorsiflexion +, plantarflexion -) in sagittal plane during a physiological human gait cycle[3]. 12

2.4 Internal moments of hip, knee and ankle in sagittal plane during a physiological human gait cycle[3]. 13

2.5 Motion capture system: from marker placement (left) to digital output in *Vicon* (right)[4]. 18

2.6 Representation of the measured forces and torques of a force plate[5]. 19

2.7 Complete free-body diagram of a single segment, showing reaction and gravitational forces, net moments of force, and all linear and angular accelerations[6]. 20

2.8 Motion capture lab with infrared cameras, reflective markers and treadmill[7]. 23

2.9 Ultrasound echoes returning from tissue interfaces (represented by black bars 1, 2, and 3) appear as peaks on the graph A-mode graph. Each peak is translated onto a screen as a dot with varying grayscale, representing the B-mode. The brightness of each dot corresponds to the amplitude of the returning echo, and its position on the screen is determined by the time it takes for the echo to return to the transducer [8]. 24

2.10 Ultrasound B-mode image with fascicle length and pennation angle. . 25

2.11 Indirect method to calculate the whole fascicle length via B-mode image [9]. 27

2.12 Definition of region of interest (ROI) and fascicle. 28

3.1 Systems involved in the experimental design with their purpose and connection. 31

3.2 Placement of HBM marker set. 32

3.3 Beamformer and transducer by *TELEMED Ultrasound medical systems*. 33

3.4 Participant on treadmill, prepared for the experiment. 36

3.5 Graph of fascicle length using key-frame correction in *UltraTrack*. . . 39

4.1 Comparison of the progression of knee and hip joint moments between Participant 3 and the rest of the participants. The solid line indicates the 0° condition, while the dotted line represents the inclined walking. The red lines are referenced to Participant 3, whereas the black ones represent the mean of all other participants. 48

4.2 Progression plot of the fascicle length (FL) per frame during an entire walking trial of one representative participant. The solid line indicates the 0° condition, while the dotted line represents the inclined walking. The vertical gray lines mark the heel-strike (HS). Ultrasound measured fascicle stretch range (*USR*) calculation is shown for both settings. . . 50

4.3 Mean progression plot of the fascicle length (FL) for a separate gait cycle in percent [%] of one representative participant. The solid line indicates the 0° condition, while the dotted line represents the inclined walking. The dashed vertical line marks the transition from the stance to the swing phase. 51

4.4 Box plots of the ultrasound measured fascicle stretch range (*USR*) data sorted from lowest to highest walking speed. Black boxes show values for non-inclined walking and gray boxes for the 10° inclined condition. For each pair $*$ indicates a p-value $< .05$, $**$ signifies $p < .01$. 52

4.5 Angle and joint moment data for ankle, knee, and hip. Angles are plotted against the full gait cycle (transition from the stance to the swing phase marked by the vertical dashed line), and moments against the stance phase are normalized to 100%. The corresponding extracted parameters (initial angle angle (*IAA*), initial knee angle (*IKA*), initial hip angle (*IHA*) and maximum plantarflexion moment (*MPFM*), maximum knee extension moment (*MKEM*), maximum knee flexion moment (*MKFM*), maximum hip extension moment (*MHEM*), maximum hip flexion moment (*MHFM*)) are drawn into the plots. 55

4.6 Comparison of the ankle parameters for all participants' means. For each pair $*$ indicates a p-value $< .05$, $**$ signifies $p < .01$. 56

4.7 Comparison of the knee parameters for all participants' means. For each pair $*$ indicates a p-value $< .05$, $**$ signifies $p < .01$. 57

4.8 Comparison of the hip parameters for all participants' means. For each pair $*$ indicates a p-value $< .05$, $**$ signifies $p < .01$. 58

4.9 Scatter plots of the initial angle angle (IAA) against the ultrasound measured fascicle stretch range (USR) during walking with 0° (left) and 10° (right) inclination, with the line representing the linear trend for each pair of parameters. The Pearson R in the upper right corner indicates the degree of correlation in the data. 61
4.10 Scatter plots of the initial ankle angle (IAA) vs the initial knee angle (IKA) during walking with 0° (left) and 10° (right) inclination, with the line representing the linear trend for each pair of parameters. The Pearson R in the upper right corner indicates the degree of correlation in the data. 62
4.11 Scatter plots of the initial ankle angle (IAA) against the maximum hip extension moment ($MHEM$) during walking with 0° (left) and 10° (right) inclination, with the line representing the linear trend for each pair of parameters. The Pearson R in the upper right corner indicates the degree of correlation in the data. 62

5.1 Comparison of the lower body joint angle progressions between the literature (left) and the study results (right). 64
5.2 Comparison of the lower body joint moment progressions between the literature (left) and the study results (right). 65
5.3 Direct comparison of the fascicle length and angle (ankle, knee, and hip) progression for participants 7, 1, and 5. The gray shaded area indicates the stance phase, while the white area marks the swing phase. 74

List of Tables

3.1 Anthropometric data for all participants 29
3.2 Settings for B-mode ultrasound 34
3.3 Description of ultrasound, kinematic and kinetic parameters later used for statistical analysis. See Figures 4.2 and 4.5 for further indication within the progression plots of the fascicle length (FL), angles and, moments. 41

4.1 Anthropometric data for participants included in the data analysis . 47
4.2 Calculated p-values for paired t-tests and the according effect sizes after Hedges' g for the ultrasound data; S = small effect ($|g| < 0.5$), M = medium effect ($0.5 \leq |g| \leq 0.8$), L = large effect ($|g| > 0.8$). The columns represent the participants included in the calculations. * indicates a p-value $< .05$, ** signifies $p < .01$. Participants 4, 5, 11, and 12 are marked, since no sign. was found for ultrasound measured fascicle stretch range (USR). ↑: increase, ↓: decrease of the parameter. 52
4.3 Mean values and results of the t-tests for the comparison of parameters between 0° and 10° incline. For each pair $*$ indicates a p-value $< .05$, $**$ signifies $p < .01$. [1]Calculated with Wilcoxon signed-rank test. . . . 57
4.4 Calculated correlation coefficients and p-values of the ultrasound, angle, and moment parameters in relationship to initial ankle angle (IAA). [2]The correlation coefficient is Spearman's ρ here. 59

Abbrevations

COM center of mass

CT computer tomography

EMG electromyography

FL fascicle length

GM gastrocnemius medialis

GRF ground reaction force

HS heel-strike

IAA initial ankle angle

IC initial contact

IHA initial hip angle

IKA initial knee angle

JWI Julius Wolff Institute

MHEM maximum hip extension moment

MHFM maximum hip flexion moment

MKEM maximum knee extension moment

MKFM maximum knee flexion moment

MPFM maximum plantarflexion moment

MRI magnetic resonance imaging

PA pennation angle

ROI region of interest

ROM range of motion

TO toe-off

US ultrasound

USR ultrasound measured fascicle stretch range

CHAPTER 1

Introduction

Hiking is the most popular active leisure activity in Austria[10]. A study from 2017 asked the population about their leisure behavior. 54% named hiking or walking as their regularly pursued exercise. 29% said they do it occasionally (2-3 times a month), and 11% of all Austrians go hiking at least once a week[10]. The popularity of hiking among humans might stem from the ability to enjoy the outdoors without deep contemplation, effectively leaving behind stress and work at home.

Mostly, the hike starts on a trail without a slope, but it will steepen to a certain level at one point. At this transitioning point from level to uphill walking, nobody will stop and think about how to adjust the posture or way of locomotion. There is no need to change one's mindset before starting this new task. Individuals who are physically and mentally capable persist in walking, and the body will naturally overcome most obstacles without requiring significant effort. However, some adjustments can be observed quite easily by everyone. For example, people will tilt their upper bodies forward because there is a need for a forward shift of the center of mass (COM) to avoid falling backwards[11].

Despite these discernible changes, many unanswered questions persist regarding

the biomechanical behavior of the body during uphill walking. Changes in posture can lead to adjustments in angles and moments within various joints, potentially prompting modifications in the musculoskeletal system, including variations in muscle utilization or unanticipated stresses. In this context, walking on an inclined level significantly increases the risk of falling compared to walking on a flat surface and the likelihood of getting injured[12]. The study of gait on inclined surfaces has long been a fundamental research focus for scientists worldwide, and there is no end to the research of variations in inclined gait. Searching the website of *PubMed®* with the terms "(gait) AND (incline)", 875 entries were found, dating from 1969 until today, with increasing tendency.

Since gait is the essential locomotion for humans, scientists use different approaches and methods to investigate it. The lower parts of the body are crucial during this exercise. Consequently, researchers frequently utilize leg muscles, as well as parameters related to ankle, knee, and hip interactions and moments, as points of comparison for various locomotive or stationary tasks (for review: [13, 14, 15, 16, 17]). Within this context, the interplay between the calf muscle and the Achilles tendon assumes a distinctive role, particularly during the stance phase of human gait[18, 19]. The gastrocnemius muscle is of particular research interest due to its unique characteristics. Being a biarticular muscle, it spans both the knee and ankle joints. This anatomical feature grants the gastrocnemius the capacity to influence two joints, potentially impacting a broader spectrum of movements and functions.

Most researchers conducting biomechanical gait analyses have primarily concentrated on level walking, while a subset has undertaken comparisons with running. Only in the past few years have research scientists also paid attention to uphill walking. Exploring this locomotion task is essential not only for general knowledge but also to gain insights into the factors behind slips and falls, the demands of rehabilitation, and the design of prostheses, as highlighted by McIntosh[20]. Additionally,

incline walking is considered a prevalent form of exercise and rehabilitation[21]. One reason could be that studies showed that metabolic power, calorie consumption, and fat-burning increase when walking on an inclined surface compared to a level one[11, 22]. Especially considering the frequent use of this mode of locomotion and the expected positive influence on metabolic and biomechanical aspects, it is indispensable to know precisely the differences between walking on flat surfaces and slopes.

Researchers employ a variety of methodologies when investigating this phenomenon. Fundamental analyses of spatio-temporal parameters such as walking speed, cadence, and stride length can be found early in the research[23]. Most studies compare hip, knee and ankle angles and moments.[24]. Further investigation of the COM[21], ground reaction force (GRF)[25], pelvic tilt[20], or rotation[26] are components of studies. Frequently, the muscles of the limb are included in the examined subjects, employing either electromyography (EMG)[27, 22] or ultrasound (US)[28] as assessment tools. In 2006, Lay et al. emphasized the need for further comparison of fascicle length with kinematic and kinetic data, as they suggested an association between kinematics and muscle length changes, an area that had been minimally researched[25]. Thus, it is helpful to use ultrasound to analyze fascicle lengths in muscles and compare them with ankle, knee, and hip data to understand their relation.

Building on several studies which compared kinematic and kinetic parameters of different participants, this thesis presents a study designed to comprehensively analyze their correlation. The study incorporates considerations of joint angles, ultrasound measurements, and discussions on joint moments. This approach aims to provide more insight whether the distal joints of the knee and hip compensate for a decreasing fascicle length and, consequently, ankle moment. To achieve this objective, a comparison was conducted between some of the most commonly

used biomechanical parameters during level walking and walking on a 10° incline. Moreover, this study aims to shed light on whether performance in this physical activity varies between uphill and level walking and to explore the underlying factors contributing to such differences.

The aim of this study is therefore to determine relationships between gastrocnemius medialis muscle fascicle length, joint kinematics, and lower limb (hip, knee, and ankle) moments during inclined walking. In order to address this, three hypotheses are formulated and tested:

1. A noticeable interaction will be identified between the gastrocnemius muscle and the joint biomechanics (angles and moments) - see Chapter 5.1 and 5.3.
2. This interaction will exhibit a pronounced shift in joint strategy when walking on an incline. Thus, it is possible to find patterns that describe specific walking strategies between groups of participants - see Chapter 5.
3. There will be an association between initial ankle angle contact and muscle fascicle length change, as well as joint angles and moments during inclined gait - see Chapter 5.3.

This thesis is divided into six chapters. After the introduction (Chapter 1), the basics of human gait, including muscle architecture of the calf and biomechanics of the involved joints, are presented in Chapter 2. This chapter also explains the role of gait analysis in biomechanical research and relates to the performed study at the Julius Wolff Institute (JWI). Chapter 3 lists and describes the materials needed for the study. Furthermore, it defines the experimental protocol, data processing, and statistical analysis. Chapter 4 introduces the results, which are subsequently discussed and evaluated in Chapter 5. Chapter 6 serves as the conclusion of the master's thesis and provides an outlook on possible adjustments to the study.

CHAPTER 2

Background

The following chapter describes the principles of human gait. That includes characterizing which body parts represent the more important ones for this locomotion. Additionally, it looks at the biomechanical role of those measures evaluated in the performed study. Lastly, it explains the two methods used for data collection.

2.1 Biomechanical Aspects of Walking

"[...] [W]alking [...] results from a complicated process involving the brain, spinal cord, peripheral nerves, muscles, bones, and joints."[3]. Despite its complexity, for most people walking is an everyday activity that needs no detailed explanation. People often walk to get around, for leisure or for sport, and the sight of people walking is a familiar sight in streets, parks and buildings. For those who have lost the ability to walk, the motivation to regain this ability is very high, as walking plays an important role in daily life by helping to overcome obstacles, complete tasks and fit into society. While walking is considered one of the most essential and yet ordinary forms of movement, its significance often goes unnoticed by those

participating in it.

Nevertheless, the systematic study of walking is also of professional importance. In recent years, human walking has been the subject of research in various fields. Biomechanical engineers, neurologists, rheumatologists, orthopaedic surgeons and physiotherapists have studied gait analysis and contributed new findings to the understanding of walking[3]. To establish a foundational comprehension of these scientific works, the forthcoming sections delineate essential background information. This includes discussions on the gait cycle, calf muscle structure, lower limb biomechanics and the systems used for gait analysis.

2.1.1 The Gait Cycle

From a biomechanical point of view, the most important players during walking are bones, muscles, and joints of the lower body, such as hip, knee, and ankle joints, and bones and muscles of the upper and lower limbs. In studies, different parameters are defined and usually compared per gait cycle. The initial contact (IC) to the following IC of one leg defines one gait cycle. Several more phases are defined and considered fixed indicators throughout research history. Figure 2.1 shows an entire cycle (0-100%) of the right leg for a physiological gait. Generally, one cycle can be divided into two main parts. One is the stance phase (60%), where the body is supported by the observed and partly by the contralateral leg. The other is the swing phase, which occurs when the observed leg is not touching the ground. The latter lasts for about 40% of the entire cycle. The two stages contain several sub-phases.

The cycle starts with the IC, also called heel-strike (HS), at 0% to 2%. The following phases during the stance phase are loading response (2-12%), mid-stance (12-31%), terminal stance (31-50%), and finally, pre-swing (50-60%), which marks the preparation for the upcoming swing phase. A toe-off (TO) marks the swing

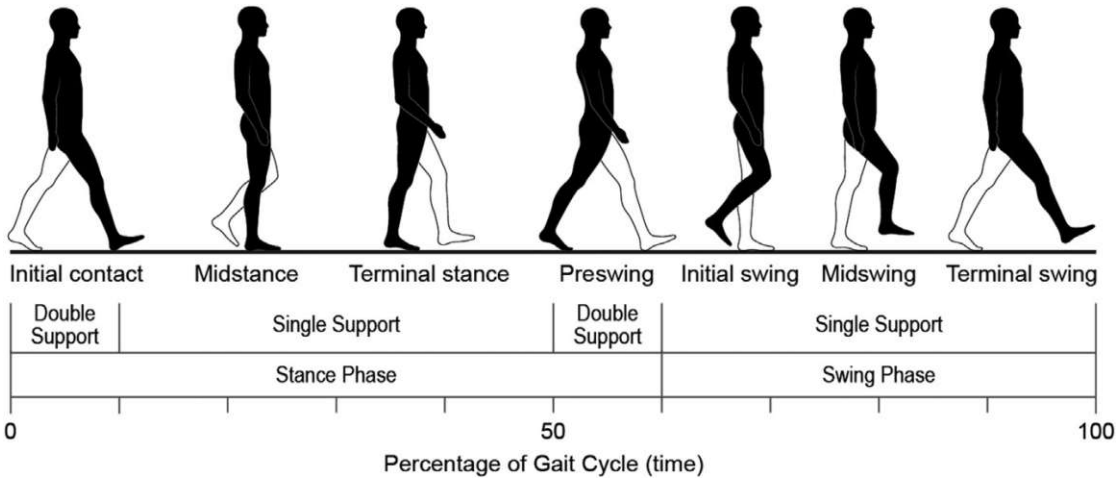

Figure 2.1: Physiological human gait cycle[1].

phase of the observed leg, followed by an initial swing (60-73%), mid-swing (74-84%), and terminal swing (85-100%)[29]. The cycle finishes with the next IC. Different body parts and their contribution are explained further in the following sections to get a more detailed insight into gait.

2.1.2 Calf Muscle Architecture

Muscles are essential during gait since everyone generally needs them for movement and support. Studies typically concentrate on the muscles of the lower body, and researchers often rely on replicated assumptions regarding their activity and interactions within the physiological gait. For example, McIntosh et al. [20] employed a marker system (for more information, see Chapter 2.2.1) that primarily concentrated on the lower extremities. Similarly, Holden et al. [30] specifically investigated the movement of the shank. Each of these studies aimed to enhance existing methodologies.

Figure 2.2 shows the stimulation pattern of selected muscles during a complete gait cycle. It is noticeable that anterior muscles (iliopsoas, vastus, tibialis anterior, extensor digitorum, and extensor hallucis) are most active during the swing phase.

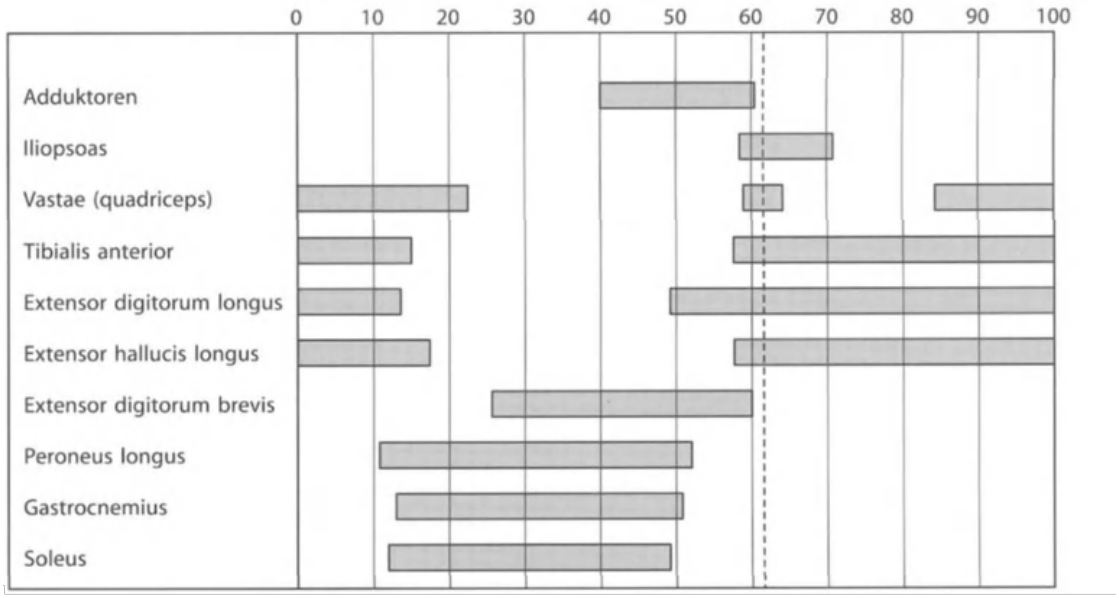

Figure 2.2: Physiological muscle interaction during one gait cycle[2].

At the same time, the lateral (peroneus longus), medial (adductors) and posterior (gastrocnemius and soleus) muscles contribute to the stance phase. The triceps surae muscle complex consisting of the gastrocnemius medialis (GM) and gastrocnemius lateralis and the soleus is supposed to have a great impact.

Both gastrocnemius and soleus are considered responsible for the plantarflexion of the ankle. Nevertheless, Neptune et al. [31] describe different functional roles during the stance phase. At the beginning of single-leg support, both muscles induce vertical acceleration to the trunk while decelerating it. During an isometric contraction, the soleus and gastrocnemius work in different directions. While gastrocnemius provides energy to the leg, the soleus decelerates it, and for the trunk, it happens vice versa. They show that not the soleus but the gastrocnemius pushes the foot forward at the end of the stance phase and generates around 93% of the force. The soleus, however, is mainly responsible for the forward movement of the trunk[31].

Looking at the anatomy of the soleus and the gastrocnemius muscles, one can easily see their connection since they both insert into the Achilles tendon, forming a three-headed muscle complex. The soleus originates in the upper third of the fibula. On the other hand, the gastrocnemius originates in the superior aspect of the medial condyle of the femur. The latter also assists in flexing the knee[32], which makes the gastrocnemius an interesting object of investigation with several approaches, such as EMG measurement or ultrasound (US) analysis (see [13], [33], or [34]). Considering that the gastrocnemius medialis is much bigger than the gastrocnemius lateralis, it is easier to examine and has more impact as an energy supplier.

In earlier studies, it was common practice to only measure activity using EMG. More recently, however, the focus has shifted to examining the processes within the muscles. The appeal lies in understanding when and how strongly the muscles contract and observing changes in muscle length, which is facilitated by the use of US technology. There are different opinions about the gastrocnemius' standard fascicle length in literature. Fukunaga et al.[18] for instance, examined the fascicle length during level walking and found that they range from 43±3 mm at TO up to 52±3 mm during the stance phase. Additionally, they discovered that a 5-9% length change can occur at any given phase from cycle to cycle. Other studies found the longest fascicle length (FL) of approximately 54 mm during HS and the shortest after TO (∼40 mm)[35].

Other publications have dealt with questions about how GM adapts to changing speed during walking[34] or angles of ankle, knee, or hip angles[36, 37, 38]. Additionally, more studies can be found where level walking knowledge is compared to new insights about GM adaptation to incline walking, primarily focusing on EMG data[39, 27] and one study including US as well[28], yet with only six healthy participants.

Lichtwark and Wilson state no significant difference in FL between level and incline walking of 10%. During mid-stance, when ankle dorsiflexion increases, they measured FL of 57.7±2.3 mm for level and 58.1±2.3 mm for incline condition. They also found the significance of fascicle shortening during the swing phase[28]. Others describe a significant decrease from 57.0±3.0 to 34.0±1.5 mm during plantarflexion, i.e., late stance phase. However, this occurs during larger flexion angles (from neutral 0° to plantarflexion of -60°)[40].

Another important aspect of muscle architecture is considering the force-length relationship within the fascicle. It describes that more or less force can be exerted depending on the length of the fascicle. Furthermore, a plateau region exists, where further elongation of the fascicle does not increase or decrease the force production[41]. That range can be considered the optimal fascicle length since it represents the peak of the force-length curve. Herzog et al.[42] state that this plateau extends from around 40 mm to 46 mm of the fascicle for the GM.

The focus of many research groups is on the complexity of muscle adaptations during gait, with an emphasis on the gastrocnemius medialis (GM). The discussion underlines the multifaceted role of the gastrocnemius medialis muscle in different phases of the gait cycle and its complex interaction with other muscles. The analyses address the variations in muscle activity and the challenges in understanding the functions of the GM even during inclined gait. In addition, the importance of using advanced technologies such as the US for a more comprehensive study of muscle dynamics is emphasized. The studies not only examine traditional EMG, but also look at muscle architecture and consider factors such as fascicle length and the force-length ratio within the fascicle, for example using ultrasound technology. The results suggest that the GM exhibits different adaptations in different individuals and under different walking conditions, challenging previous assumptions

and highlighting the need for a nuanced understanding of muscle behavior during walking.

2.1.3 Biomechanics of the Lower Extremities

As stated before, the lower body joints significantly impact human walking besides muscles. A physiological gait cycle will highlight the progression of the ankle, hip, and knee angles and moments. That gives fundamental insight into how hip, knee, and ankle joints influence the gait pattern of an individual.

Level walking

As seen in Figure 2.3, the hip flexes at around 25° from a sagittal perspective during the HS[1]. During progressing gait, flexion decreases until a neutral position of the hip is reached at around 27% of the gait cycle, just before mid-stance. At pre-swing, the maximum extension emerges at approximately 20°. The leg moves forward, reaching a neutral hip position during the initial swing phase until maximal hip flexion of about 30°, finishing the second arc of hip movement [1].

The middle graph in Figure 2.3 displays the knee angle. The knee is "essential for lower limb advancement," thus playing an essential role during the gait [1]. Physiologically examined, the knee flexion angle starts at around 3-5° at HS while absorbing shock during the following short phase. Angles reach the first maximum in the early stance and decrease until the terminal stance, where the knee is almost fully extended. Here, the knee "provides stability for weight-bearing throughout the stance." [1]. From that point on, angles increase again until the knee reaches maximum flexion of approximately 60-70° during the initial swing phase to initialize the forward movement of the lower limb and lift the toe above the ground. Sheffler

[1]Please note, that the displayed angle represents the angle between the thigh and the vertical axis. According to the book of Whittle the pelvis movement in the sagittal plane is so small, that it has almost no influence on a different outcome [3].

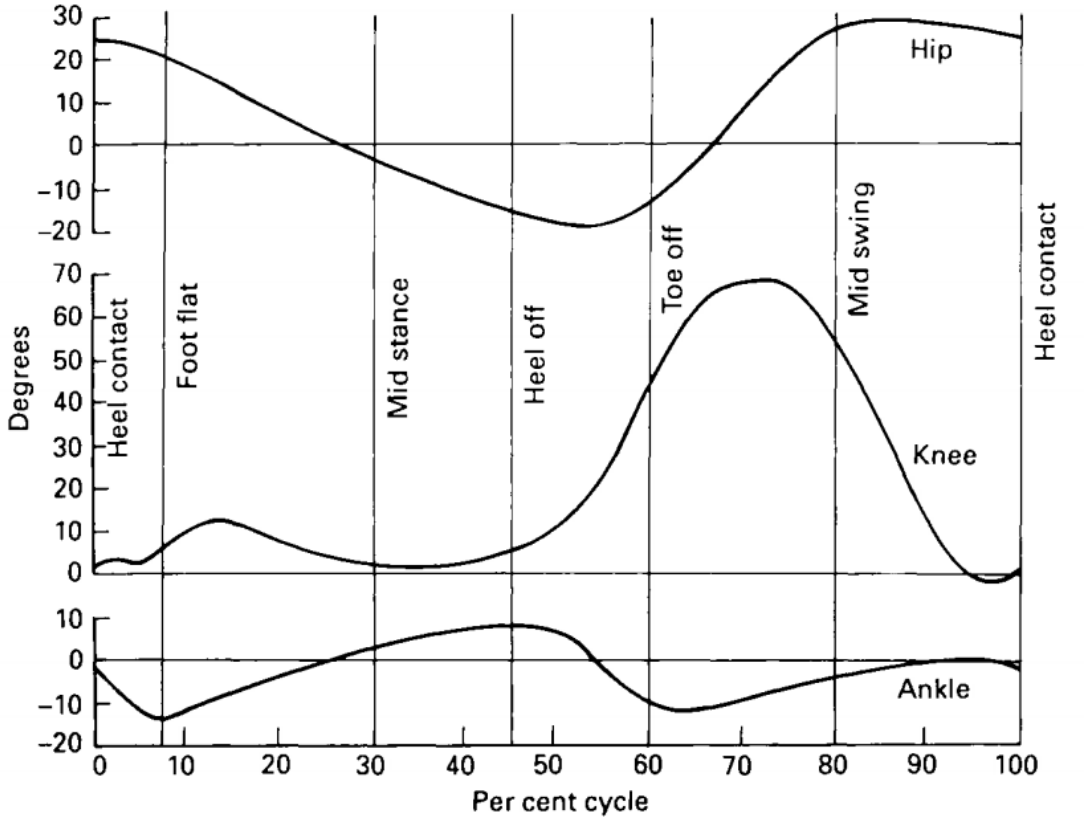

Figure 2.3: Angles of hip (flexion +, extension -), knee (flexion +, hyperextension -) and ankle (dorsiflexion +, plantarflexion -) in sagittal plane during a physiological human gait cycle[3].

and Chae[1] state that "[...] in normal walking, 60° of the ipsilateral knee flexion are needed to achieve toe clearance." After the peak, the knee angle decreases with the same steepness as it rose until even small hyperextension can transpire before the subsequent HS.

The ankle moves through four arcs of motion during a complete cycle. During HS, the ankle is slightly plantarflexed in an almost neutral position. Plantarflexion increases to approximately 15° until flat foot position. The ankle angle slowly increases during the following single-support stance until its global dorsiflexion peak is reached at around 10° before the heel-off. This period is considered very

important for the progression of the tibia and finishes the second arc of ankle motion[1]. Following, the ankle progresses to plantarflexion until a local peak is reached right after TO, where the leg pushes forward. That is induced mainly by the gastrocnemius (see Section 2.1.2). The ankle needs a final movement to dorsiflexion to gain foot clearance.

In the analysis of the joints, not only the angles are a vital parameter, but also

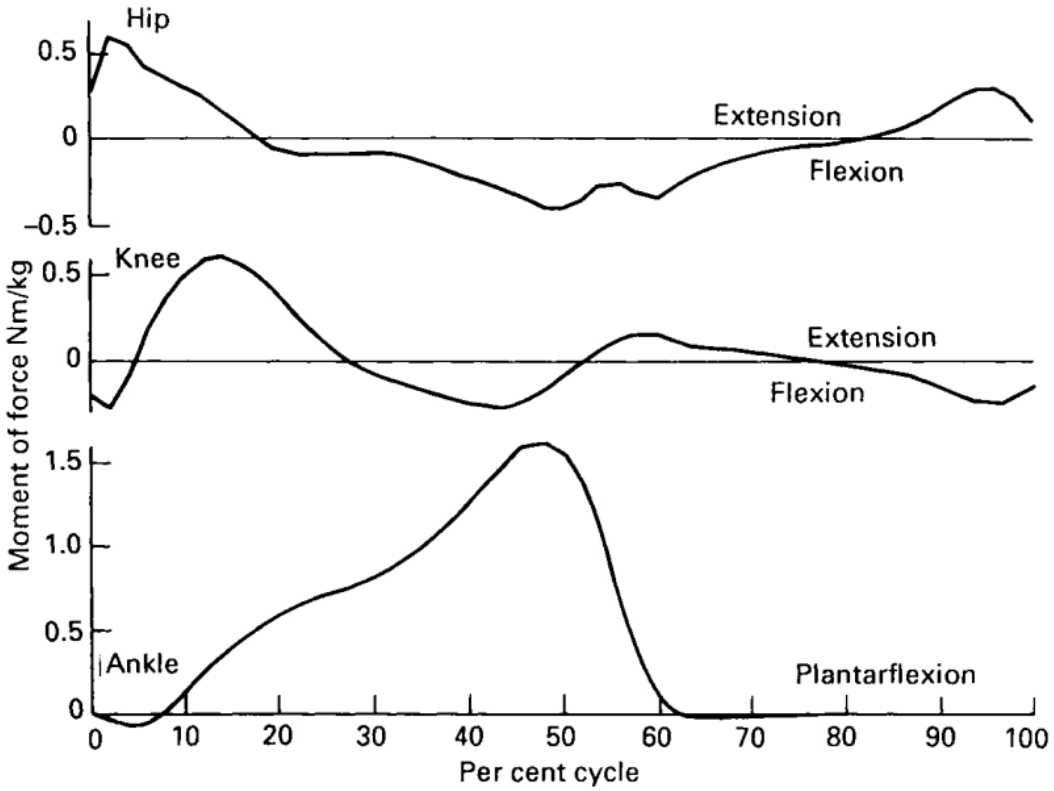

Figure 2.4: Internal moments of hip, knee and ankle in sagittal plane during a physiological human gait cycle[3].

the internal muscle moments. Those are visualized for a physiological gait and normalized to body weight in Figure 2.4.

Throughout the stance phase, when the leg is extended, the curve gradually transitions towards its negative maximum (flexion moments) at heel-strike, which is

mainly caused by the eccentric contraction of the iliopsoas. Another peak extension moment during the end phase of the gait cycle is generated primarily by the hamstring to prevent any further flexion of the hip[3].

Internal knee moments in the middle of the three graphs, show a different course, although maximum extension moments have a similar magnitude. A flexion peak occurs before an extension peak because of the hamstring's contraction, preventing knee hyperextension during the foot-flat stage. While the knee flexes, the quadriceps produce an internal extension moment and peaks between loading response and mid-stance. Likewise, it changes to flexion moments while the knee extends again. The GM primarily induces the following flexion moment peak at heel-off and marks the repeated transition towards flexion, thus extension moments. Another last change occurs at the end of the swing phase, again by the hamstring contraction[3].

The ankle moment has the most distinctive shape and is more significant than the hip and knee moments. Ankle moments start with a sharp negative peak (dorsiflexion) like knee moments. Plantarflexion moments arise after this short period until they reach their maximum at more than $1.5\frac{Nm}{kg}$. That is because gastrocnemius and soleus contract, generating high internal forces and moments to release any moments when the foot leaves the ground. The tibialis anterior induces only a tiny dorsiflexion moment to keep the foot lifted[3].

The measures of angles and moments are common knowledge and can be found in many books, with minor differences in magnitudes or course and with varying sign conventions. In summary, level walking conditions have been repeatedly investigated and shown similar results throughout studies. Beyond walking, it has been also an objective to get insights into how the human body adapts to other gait conditions, such as running or inclined walking. The motivation for conducting such studies is twofold: biomedical researchers can gain additional insights into the mechanisms and principles of walking, while practitioners can gain knowledge for

rehabilitation.

Incline walking

Scientists have found significant differences in joint angles and moments when comparing level to incline walking. However, the studies reviewed in this thesis are not in complete agreement: Lay et al.[25], McIntosh et al.[20], and Haggerty et al.[21] found significant differences between level and incline walking in the ankle, knee, and hip angle at heel-strike, peak knee angle at the stance phase as well as peak ankle angle at mid-stance for 15% incline and 10° respectively (McIntosh et al.).
Nonetheless, only Haggerty et al. report differences between level and incline walking in peak hip angles during stance[21]. All three groups show significance in peak hip-extensor moments in early stance and ankle plantarflexion during terminal stance. In contrast, Lay et al. did not report any differences in maximum extensor moments of the knee in loading response[25]. Questions remain, after all, how these found variations influence or are affected by specific muscles or other body parts.

A crucial influence of the lower body joints on human walking is evident, with the angles and moments of the ankle, hip and knee playing an important role throughout the gait cycle. In the context of level walking, the flexion and extension patterns of these joints are particularly important, suggesting that this interaction is also relevant when walking uphill. Internal muscle moments provide additional insight and show patterns such as a sharp negative peak in dorsiflexion followed by plantar flexion moments generated by the gastrocnemius and soleus. While these measures are well established in level walking, there is disagreement among research groups in the transition to uphill walking. Lay et al.[25], McIntosh et al.[20] and Haggerty et al.[20] report significant differences in joint angles and

moments during uphill walking, but are not in complete consensus about their outcomes. This shows that questions remain about the specific muscles or body parts affected by these changes and how they adapt their interactions, highlighting the need for further research in this area.

2.2 Gait Analysis in Biomedical Research

Biomechanics research uses advanced techniques to understand the intricacies of human movement and gain valuable insights for both scientific understanding and practical applications. Among these techniques, motion capture and ultrasonography play a central role in detecting and analyzing the complex biomechanical processes. Motion capture with specialized cameras and markers enables precise tracking of body movements and facilitates the assessment of joint angles, muscle activity and overall kinematics during various activities. On the other hand, ultrasonography allows researchers to explore the structural dynamics of muscles and tendons in real time, offering a detailed overview of length changes and morphology during movement. A more detailed explanation of the two approaches is provided in the subsequent sections.

2.2.1 Motion Capture

Analyzing the kinematics of human gait has been an interest for centuries. The most straightforward approach is watching someone walk in a lab and try to see anomalies or differences. This method developed into more complex methods with a variety of technologies. In the beginning, already in the 1870s, scientists used photography to capture movement. Not until about 100 years later, electronic devices, like video cameras, replaced this method to gain more precise data[3]. However, all these techniques share the same principles: attaining information

about human motion by capturing, quantifying, and comparing it.

In biomedical research, the human body diverges into rigid segments, the number depending on the interest of investigation. For example, in gait analysis, six main segments are often selected: left and right foot, left and right calf, and left and right thigh[43]. To investigate movement, one must know each segment's position and orientation in space and time. From this information, respective linear and angular velocities and accelerations can be calculated as well. For a 3D space, six independent coordinates must be recorded for each segment: three cartesian coordinates (X, Y, and Z) and three angles of rotation, that represent translation and rotation around the center of mass of the segment[43].

One much-used method to obtain this information requires at least three reflective markers, which are placed on representing structures of each segment of the studied participant. The proper placement and amount of markers have been widely investigated, and many different methods are used, each having advantages and disadvantages[43]. Users select them according to application and personal preference. It is recommended to affix the markers on specific landmarks near a rotation center to ensure comparability across studies[3]. That could be, e.g., on the skin right over the medial and lateral condyles of the femur when representing the distal end of the thigh and the proximal end of the calf segment.

In a laboratory setting, infrared strobe cameras are strategically positioned so that, during any participant's movement, each marker is captured by more than one camera, ensuring a continuous 3D perspective of the segments[3]. The infrared light is sent out stroboscopically, reflected by the markers, and captured by the cameras. All cameras need to be synchronized and calibrated before use.

A connected computer and softwares, such as *Visual 3D* (*C-motion Inc.*, USA), reconstruct each marker's correct position and orientation in 3D space. Subsequently, each segment can then be modeled and used for further investigations. Depending

on the software used and the purpose of use, there are various approaches to modeling, such as AnyBody, OpenSim or the Human Body Model (HBM)[44]. To compute the joint angles as outlined in Section 2.1.3, it is essential to establish the orientation of the segments relative to each other. As described above, "[e]ach joint has a reference frame in the proximal and distal segments (for the hip joint, this is the pelvis and thigh; for the knee joint, the thigh, and the calf; for the ankle joint, the calf and foot)"[43]. Thus, the angles are the rotation of the defined distal segment relative to the proximal one. In the sagittal plane (about the z-axis), these rotations are called flexion and extension for the hip, knee, and ankle, referred to as dorsi- and plantarflexion[43]. Figure 2.5 shows how the markers attached to the body are reconstructed digitally and further processed to build up different segments.

The previous section explained that the angles of the three main joints involved

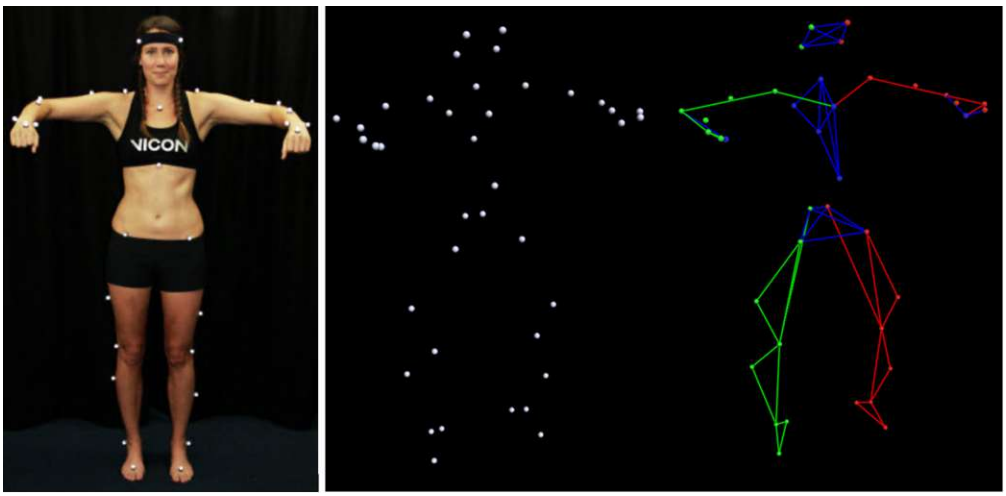

Figure 2.5: Motion capture system: from marker placement (left) to digital output in *Vicon* (right)[4].

during walking and the respective moments are crucial. Consequently, the motion capture system of markers and cameras must be extended by devices that can measure forces. Typically, in gait labs, force plates are used for this purpose. They

are mounted on the ground or on a device that people walk on, e.g., a treadmill. A state-of-the-art force plate (see Figure 2.6) can measure several components: three components (F_x, F_y, and F_z), three rotational moments (M_x, M_y, and M_z) for all three planes (sagittal, frontal, and transversal)[3]. F_x, F_y, and F_z are called ground

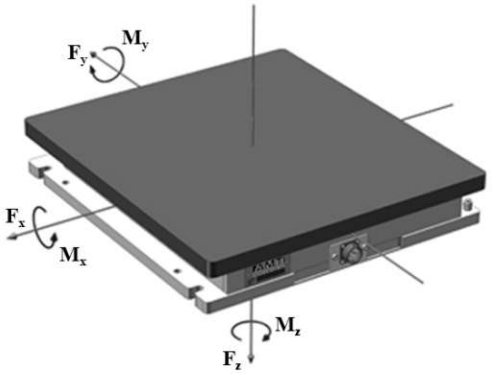

Figure 2.6: Representation of the measured forces and torques of a force plate[5].

reaction forces (GRF) because they occur by contact between the body and the floor. These values can be used to calculate the internal forces in the joints as they pass through the body from one segment to another. This process is facilitated by an inverse dynamic approach. "The conventional use of inverse dynamics involves an iterative solution of the body segments' equations of motion, which starts with measured ground reactions and, beginning with those segments in contact with the ground, calculates joint forces and moments at each successive segment."[45] An equation system, is utilized to determine net joint moments, net joint powers, and net joint intersegmental forces. This process unfolds sequentially, starting from the ankle joint and progressing to the knee and then to the hip joints. Manual calculations involving free body diagrams for each segment, as outlined by Vaughan et al.[43] and Winter[6], can be employed for this purpose. Figure 2.7 illustrates such a diagram, displaying all the known and unknown parameters. Alternatively, a more contemporary approach involves computer software applications like *Visual*

3D (*C-Motion Inc.*, Germantown, MD, USA) for these calculations.

The traditional way of using passive, reflective markers and infrared cameras in a large room where participants walk from one side to another and hit the force plates in the ground entirely only by chance has been enhanced and changed recently. Instead of markers that only reflect the light sent out, active markers that emit infrared light directly from LEDs can be used. The benefit of this method is that no post-processing step is needed, where the spots recorded by the cameras need to be tracked to the suitable marker. The drawback, however, is that participants must carry a power supply, which may include cables. Additionally, this system is

Known

a_x, a_y = acceleration of segment COM
θ = angle of segment in plane of movement
α = angular acceleration of segment in plane of movement
R_{xd}, R_{yd} = reaction forces acting at distal end of segment, usually determined from a prior analysis of the proximal forces acting on distal segment
M_d = net muscle moment acting at distal joint, usually determined from an analysis of the proximal muscle acting on distal segment

Unknown

R_{xp}, R_{yp} = reaction forces acting at proximal joint
M_p = net muscle moment acting on segment at proximal joint

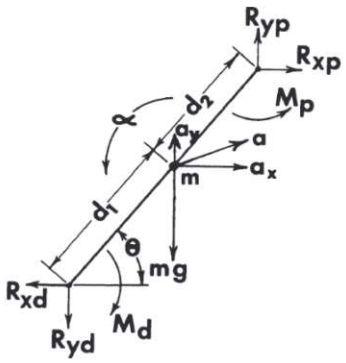

Figure 2.7: Complete free-body diagram of a single segment, showing reaction and gravitational forces, net moments of force, and all linear and angular accelerations[6].

more vulnerable to errors due to other light sources[3]. The passive system copes with that by mapping other light sources during the calibration.

The use of marker-less systems is even more advanced but still in development status. Without further preparation, they use the image data and a given model to determine the joints' position, orientation, and configuration[46]. Thus, participants of motion capture studies do not need any other technology attached to their bodies and can move freely. However, is has not been investigated whether the inclusion of additional measurement devices, such as an ultrasound device on one leg within the field of view, can have a negative impact on markerless motion detection. Therefore, this approach was not considered in this study.

The more common way of capturing the GRF is with force plates mounted onto the ground in a linear arrangement. Participants walk up and down a pathway and eventually hit them. One noteworthy disadvantage is that it can take much time until a few reasonable steps are measured since only those are useable, where the whole foot lands on the plate. Moreover, because the position of the plates can be seen quite easily, participants tend to elongate or shorten their stride length just to hit the force plate completely. Thus, bias gets incorporated into the data. To avoid this problem, increasingly, studies can be found that use treadmills instead of overground walking. The treadmill belt is split in the middle, parallel to the walking direction. Each side contains one force plate to record a single foot individually. Papegaaij and Steenbrink describe several advantages in their white paper 2017(see [47]). They state that foot placement does not need to be as accurate as in overground walking labs since the whole foot is almost with every step placed entirely on the force plate - this is not the case when feet cross over to the other side of the body. Also, more data can be acquired in a shorter time. Furthermore, treadmill walking allows users to investigate motion during a specific and constant walking speed or quickly change the speed or incline. However, treadmill walking

is an unfamiliar task for many people, which could also introduce bias to the data due to adjusted walking patterns.

Even though no study found clinically relevant differences in kinematics comparing overground to treadmill walking, three studies discovered that there are significant differences in the braking GRF, as well as the moments in the knee and hip[48, 49, 50]. Hip flexor and knee extensor moments tend to be smaller, while hip extensor and knee flexor moments show higher values in treadmill compared to overground walking. Thus, working with a treadmill, these differences need to be acknowledged. Figure 2.8 shows a modern setup in a gait lab with a treadmill. Eight infrared cameras capture the motion of the reflective markers stuck to the participant's body. Thus, each marker is visible for at least two cameras during any exercise. Digits 1 and 2 represent the two force plates mounted on the treadmill.

Motion capture systems find applications beyond basic science. They play a crucial role in rehabilitation processes and clinical practice, aiding in the treatment of conditions such as amputations, cerebral palsy, and various diseases. These systems are utilized in motor control and neuroscience departments, sports science, and even military[3, 51]. Here, the involved patients and users will immediately gain a benefit. Likewise, with the deep investigation and data assemblage, the benefit will be available to others regarding extended knowledge or possible treatment[3].

Whittle's book states: "In analyzing data from patients, it is always necessary to have an adequate baseline of normal data."[3] Thus, fundamental scientific gait analysis always needs to be done to develop information that can help in all other fields of application.

2.2.2 Ultrasonography

Many technologies exist to examine and study skeletal muscles in a healthy, pathological, or traumatic state. Ultrasonography (US) proved efficient and is commonly

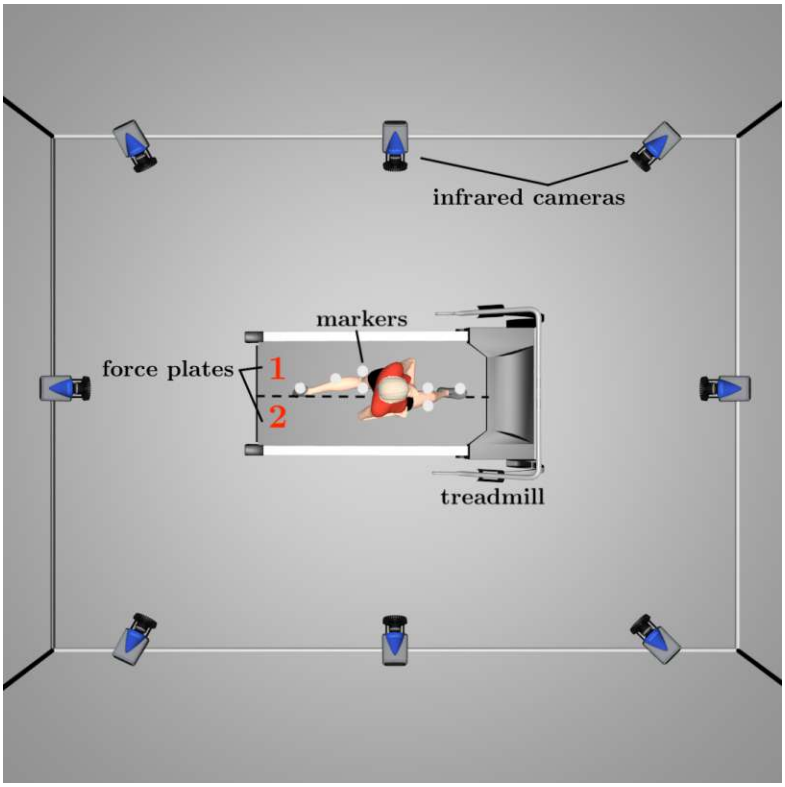

Figure 2.8: Motion capture lab with infrared cameras, reflective markers and treadmill [7].

preferred over X-radiography, computer tomography (CT), or magnetic resonance imaging (MRI). The popularity has grown because it is cheap, has high variability in size and application, and does not expose users or other involved people to radiation like CT or X-radiography. Moreover, US can supply real-time images of living tissue, which is helpful in clinical applications [52].

The most widely obtained parameters are "pennation angle (PA), muscle thickness (MT), fascial length (FL) and cross-sectional area (CSA)," as well as fascicle curvature, muscle size, and fascicle orientation [52]. Different techniques exist within this technology depending on which information users are curious about. In biomedical research, 2D brightness mode (B-mode) has been found most helpful in gaining information about any interaction in the muscle [16, 17, 18]. In this technique, a

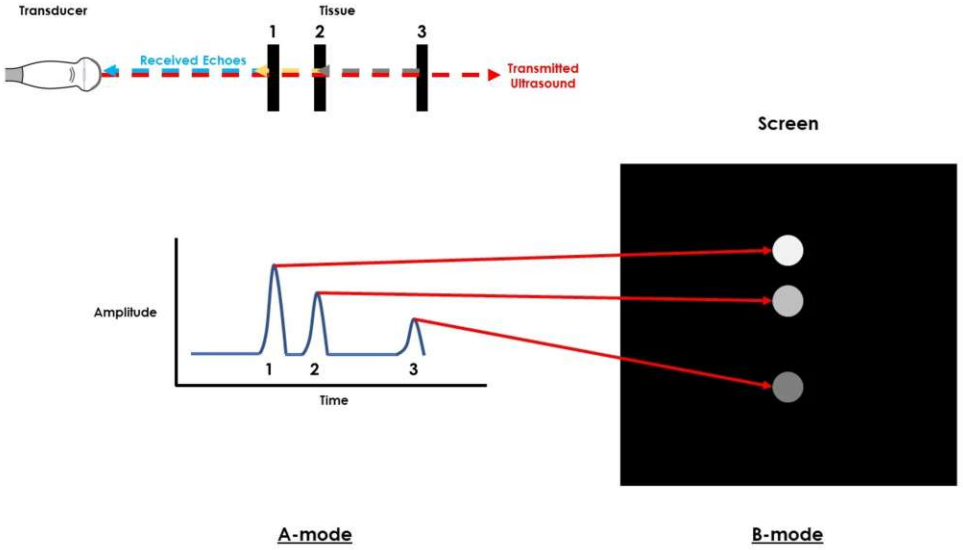

Figure 2.9: Ultrasound echoes returning from tissue interfaces (represented by black bars 1, 2, and 3) appear as peaks on the graph A-mode graph. Each peak is translated onto a screen as a dot with varying grayscale, representing the B-mode. The brightness of each dot corresponds to the amplitude of the returning echo, and its position on the screen is determined by the time it takes for the echo to return to the transducer[8].

linear array of transducers performs simultaneous scanning, transmitting a 2D image of the scanned area. The method is supposed to have similar outcomes as CT or MRI. Moreover, it enables real-time visualization of a cross-section of muscles or other structures.

Figure 2.9 depicts the fundamental technique of B-mode US and provides a brief overview of how it differs from the more basic A-mode. Echo impulses in the ultrasound range (20 kHz to several GHz) penetrate the body and are deflected, absorbed, or reflected. What occurs depends on the impulse's wavelength and the acoustic impedance of the objects they pass. All reflected pulses, in turn, are picked up and converted by the acoustic transducers, creating an image that contains lighter or darker areas. The reflection coefficient, i.e., the number of echoes returned to the transducer which determines the object's brightness, primarily depends on

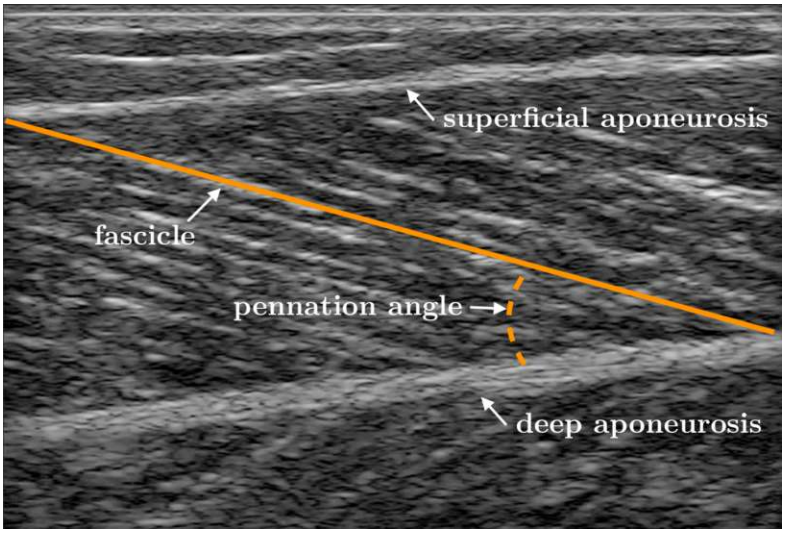

Figure 2.10: Ultrasound B-mode image with fascicle length and pennation angle.

the respective acoustic impedance and the angle of incidence of the rays[53]. In addition to the appropriate choice of wavelength, it is critical how the transducer is positioned on the examined object's surface. Another consideration must be that internal movements can cause deflection and thus distortion of the image, for example, when a muscle stretches during scanning[53].

Air is the substance with the lowest acoustic impedance in medicine, and bone has the highest. Since skeletal muscles have a high water content, they are dark structures in the B-mode US. If scanning occurs longitudinal to the muscle belly, the associated fascicles are white lines, making the muscle easy to examine[53].

Therefore, obtaining data from the B-mode images, e.g., FL and pennation angle (PA), takes effort. Figure 2.10 shows an image of the GM recorded via the B-mode US. Both superficial and deep aponeuroses are visible, and parts of the muscle. The drawn-in line represents one fascicle from which users can retrieve the length. The angle between the fascicle and the deep aponeurosis is the accompanying PA to the fascicle.

As noted before, several values are possible to obtain using US. However, one of

the most important ones is the FL if the investigation of muscle forces is intriguing. Watkins says in his book: "The amount of work done by a muscle in a concentric contraction is the product of the muscle force and the distance over which the musculotendinous unit shortens"[32]. Thus, the length change of the fiber can provide information about the capability of muscle to generate force. Several studies showed that with knowledge of the fascicle length and their changing behavior, explanations about the muscles' force-length relationship, shortening speed, or similar parameters could have been made[54, 55]. Zhou and Zheng conclude that "[t]o examine the dynamic function of muscles during contractions and movement, it is necessary to examine the length changes of the muscle fibers themselves"[52]. Thus, measuring the FL using B-mode makes gaining information about muscle behavior in different situations easy.

However, using the described technology only sometimes immediately leads to the desired results. Two main methods are described in Zhou and Zhengs' book to measure the exact FL: indirect and direct.

The indirect method occurs when the image of the US technology cannot record the whole fascicle in one picture. Thus, the remaining portion is out of view (l_2) and must be calculated and added to the visible part (l_1). The PA α, as well as the remaining thickness of the muscle h, is used to calculate l_2[9, 52]:

$$l_2 = \frac{h}{sin\alpha} \tag{2.1}$$

That leads to:

$$L_f = l_1 + l_2 = l_1 + \frac{h}{sin\alpha}. \tag{2.2}$$

Figure 2.11 shows an example calculation of the whole fascicle length using the described indirect method. However, the indirect calculation of the FL assumes that fascicles are straight and no curvature exists. Scientists observed that this is not true for muscles since curvature can be close to both aponeuroses[56]. Thus,

indirect methods can lead to errors in FL estimations.

Even more complex methods show limitations, like computation with the extended

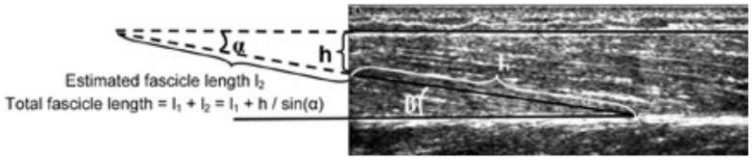

Figure 2.11: Indirect method to calculate the whole fascicle length via B-mode image[9].

field-of-view ultrasonography (EFOV US), which cannot obtain images of contracting muscles[52]. Nonetheless, a widely used technique uses a design first described by Cronin et al. in 2011[33]. Their approach is based on the Lucas-Kanade optical flow algorithm with an affine optic flow extension, automatically tracking the fascicles[33]. This method can simultaneously change length with changes due to rotation[52]. Thus, the FL measurement is possible during any dynamic movement within the muscle.

The algorithm utilizes the affine flow model to compute the flow pattern between two consecutive images. To initiate this process, predefined points in a representative image are required. Therefore, users need to manually select the region of interest (ROI) and the fascicle under investigation before starting the actual calculations. For this step, an image displaying the total length should be selected. In Figure 2.12, the selection of a ROI is shown with a dotted line, defined as "the area between the superficial and deep aponeuroses". The solid line defines the fascicle, described as "the straight line distance between the superficial and the deep aponeuroses parallel to the lines of collagenous tissue visible in the image"[33]. Six parameters are specified for the use of the affine flow model. These include the optic flow in two directions, rates of dilation and rotation, and two shear parameters. With these parameters, it is possible to calculate the affine transformation, providing an estimated flow vector of how positions v_x and v_y of specific points x

and y change. When applied to the endpoints of the defined fascicle (circles in Figure 2.12) in the subsequent image, they will be accurately defined based on the movement in the muscle[33, 52]. The user gains a continuous calculation of

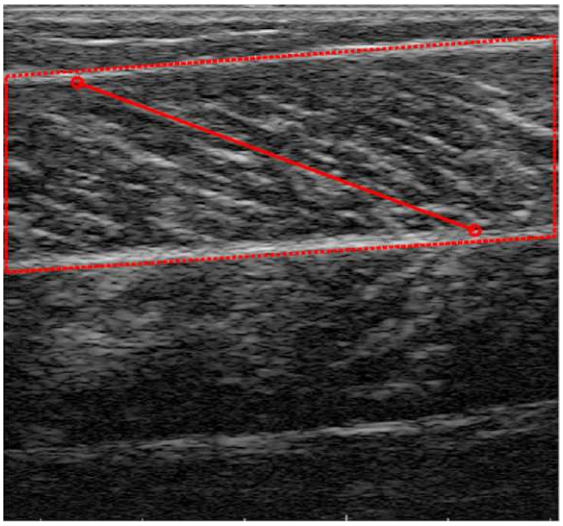

Figure 2.12: Definition of region of interest (ROI) and fascicle.

the FL during the whole recording while evaluating each frame successively. Zhou and Zheng further state that there are two advantages of this method. One is the stability against drift errors, which would be the case when small ROI are investigated instead of large muscle parts. Furthermore, using the affine flow transformation, it is possible to track fascicles even when their endpoints move out of the picture during the dynamic changes of the muscle.

CHAPTER 3

Methods

The data collected for this master's thesis is part of a larger project aiming to compare participants with and without an Achilles tendon rupture (see [57]). For reasons of clarity, only the methods that are relevant to the reported results are presented here.

3.1 Participants

Fifteen healthy male participants (age: 30.4 ± 4.8 yr, height: 178 ± 9 cm, body mass: 70.9 ± 10.7 kg; M ± SD, see Table 3.1) voluntarily participated in the study. Factors excluding participation were previous ruptures of the Achilles tendon,

	Age (years)	Stature (cm)	Weight (kg)
Mean	30.4	177.87	70.87
SD	4.82	9.35	10.73

Table 3.1: Anthropometric data for all participants

major injuries on feet and leg bones, ligaments, tendons, and neurological problems

with the lower extremities. Also, no individual with metal implants or large leg tattoos were allowed to partake in the study, since the larger study also involved an MRI scan of both legs and feet in another session. Prior to measurements, all participants gave written consent that they were informed them about the investigation's aim, background, and risks. A local ethics committee approved the study, consent, and preparation before the study started.

Previous research has demonstrated that shoes have an impact on spatial-temporal parameters[58], as well as the kinematics and kinetics of the lower body, in comparison to walking barefoot [58, 59]. However, it was assumed that participants would find wearing shoes more comfortable on the treadmill surface, thus adopting a walking style as close as possible to their natural gait. Since no scientists found significant differences between shoes of the described parameters, all participants were wearing their preferred, usual footwear for outside exercises, such as running shoes.

3.2 Experimental Design

The gait lab laboratory of the JWI in Virchowweg 23, 10117 Berlin, has a collection of devices for recording and analyzing motion data. The Gait Realtime Analysis Interactive Lab (*GRAIL*) system (manufactured by *Motek Medical B.V.*, The Netherlands) was crucial for the research project. The setup comprises a dual-belt treadmill powered and controlled by the *D-Flow* software[60] from the same manufacturer, along with an infrared camera arrangement (manufactured by *Vicon Motion Systems*, UK) and an ultrasound device (manufactured by *TELEMED*). Figure 3.1 provides an overview of the variables captured by the systems and their interconnections. Additionally, photographs and illustrations depict the configuration of the lab. The subsequent sections elaborate on the utilized systems

and their respective functions for the study.

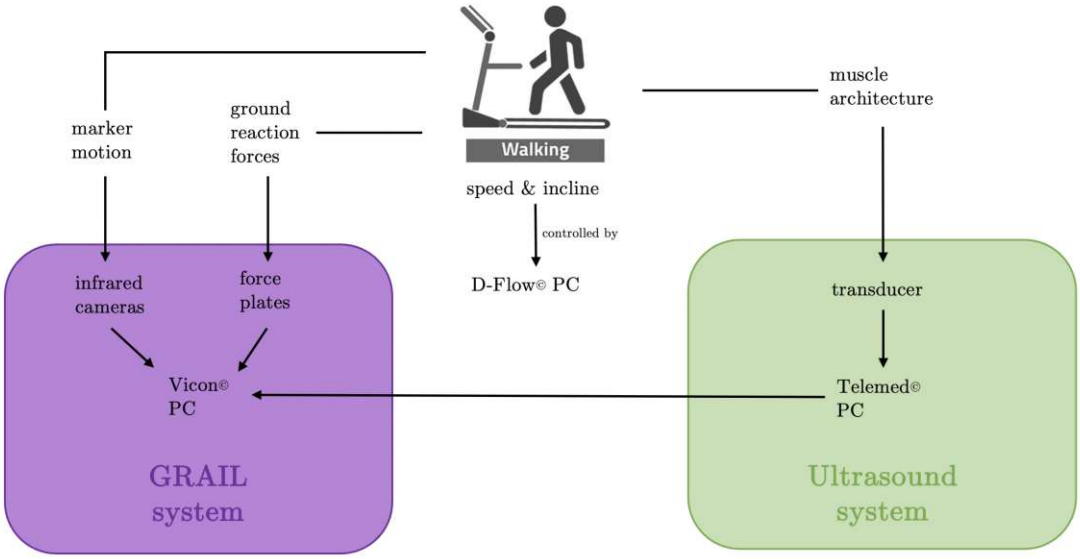

Figure 3.1: Systems involved in the experimental design with their purpose and connection.

3.2.1 GRAIL System: Joint Kinematics and Kinetics

The GRAIL and camera system was used to collect data regarding motion capture and, therefore, joint kinematics. Fourteen infrared cameras operated at 100 Hz frame rate were arranged around the treadmill to capture motion from every direction. The cameras were controlled centrally via the software *Nexus 2.8* (manufactured by *Vicon Motion Systems*, UK) on the connected computer. We worked with the Human Body Model (HBM) lower body model (see Figure 3.2 and appendix) which contains 26 markers for marker placement. In addition, three markers were attached to the US frame tied to the participants' legs, which will be described further in Chapter 2.2.2. We also employed the Nexus software to visualize the force magnitudes and directions recorded by the two *Motekforce Link* force plates integrated in parallel on a single belt and the treadmill. These plates operate at

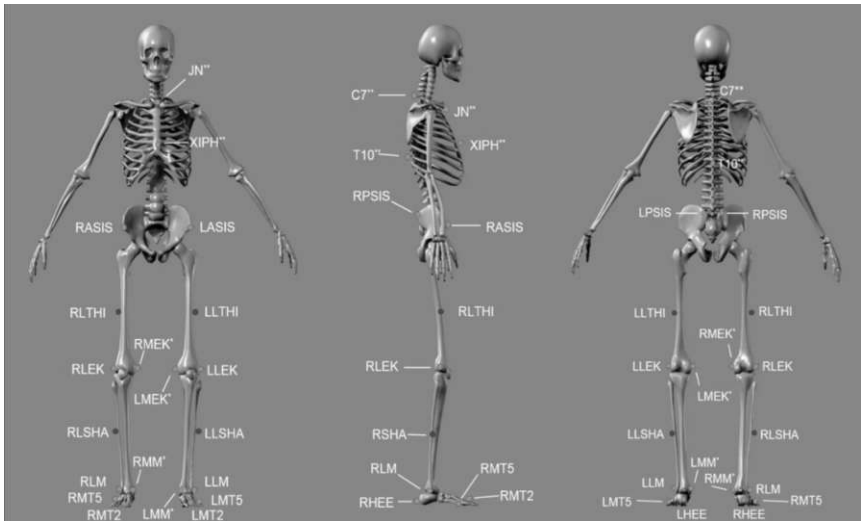

Figure 3.2: Placement of HBM marker set.

a frequency of 1000 Hz, measuring the GRF for each leg in the longitudinal (x), transversal (y), and vertical (z) directions. A 180° white semi-cylindrical screen equipped with projectors allowed for the projection of visual stimuli in front of the participant. Both the treadmill and projectors were controlled through the *D-Flow* system.

Before the actual testing, the measuring system had to be calibrated. For successful calibration, it is imperative to replicate the lighting conditions in the room as they were during previous tests. The activation of the cameras, connection systems, and computers occurred only after ensuring that specific light sources in the room were switched on to replicate identical lighting conditions. We performed the assisted calibration using *Nexus*. First, the software created a mask for each camera. Reflective objects had to be removed from the cameras' field of view. *Nexus* protects against recording reflecting locations, such as shiny metal or mirrors, to prevent detection of artifacts during testing. The recording system is then calibrated to a smaller area around the force plates. During this step, a T-shaped metal rod equipped with multiple active markers was utilized. The calibration

(a) Beamformer ArtUs EXT-1H [61] (b) Transducer LF9-5N60-A3 [62]

Figure 3.3: Beamformer and transducer by *TELEMED Ultrasound medical systems*.

process involves the person swinging the T-shaped metal rod through the air within the specified area until each camera captures 9000 images. At this point, the software can establish a global coordinate system. The metal rod then had to be placed at a marked position on the treadmill, which *Nexus* used as the system's central point.

3.2.2 Ultrasound System: Muscle Architecture

For the investigation of joint kinematics and kinetics, US technology were used to assess the muscle architecture of the GM. To capture US images, we employed the real-time sonograph system manufactured by *TELEMED Ultrasound medical systems* together with the ArtUs EXT-1H beamformer with an installed I/O module (see Figure 3.3a) and the LF9-5N60-A3 linear flat transducer (see Figure 3.3b). We connected the US probe to a computer via USB 3.0 and the *Vicon* system via the "ScanStart output" plug to synchronize US data to the gait trials at 1000 Hz. All images were obtained using B-mode ultrasonography at a frequency of 7 MHz and a depth of 50 mm. Additional settings, which can be set and changed in the *Echo Wave II* software provided by *TELEMED*, are listed in Table 3.2. The settings were found through analysis and testing prior to the actual start of experiments. After adjusting the system, the probe was positioned normally to the skin surface of the participant's medial calf. Using the live images displayed in the *Echo Wave*

II software, it was aligned along the median long axis of the GM with the cable side up, in an attempt to find a mid-belly position. A few basic rules were followed to obtain good images for accurate FL and pennation angle analysis, adopted by Bolsterlee et al.[63]:

1. "[...] the attachment of the fascicles on both aponeuroses must be visible [...]."

2. "[...] the image is perpendicular to the aponeurosis at the point of attachment of the fascicle to the aponeurosis."

They recommend rotating and tilting the probe until the aforementioned two criteria are fulfilled. Once archieved, we used a bespoke 3D-printed mounting device to fix the probe onto the participants' legs. The US head position was kept as steady as possible using straps, while the use of cushions avoided bruises.

B-Mode Control	Value
Frame Rate (FPS) in x/y	46/48
Depth (De)	50 mm
Dynamic Range (DR)	78 dB
Power (Pw)	-11 dB
Gain (Gn)	68%
Frequency (Frq)	7 MHz
Lines Denisty (LnDens)	Standard (St)
Frame Averaging (FrmAvg)	0
Rejection (Rej)	12
Image Enhancement (ImEnh)	4
Speckle Reduction NeatView Level (NV)	4

Table 3.2: Settings for B-mode ultrasound

3.3 Experimental Protocol

After providing instructions and signing the consent, participants changed into appropriate sportswear. We measured their height and weight. Each participant completed a questionnaire about their average amount and type of fitness activities during the week (see appendix). Additionally, we inquired whether they had encountered significant injuries or experienced episodes of pain in their legs during exercise. Then, the preparation started with adding the markers and the US probe. For each participant, the following protocol was carried out two times - once recording data of the left calf, and then again for the right. At all times, one lab assistant recorded kinematics data at the *Vicon* while another recorded US data. Both lab assistance were in the same room as the participant.

After being offered and possibly equipped with a voluntary safety harness, participants then stepped onto the flat treadmill. Figure 3.4 shows one participant prepared for the experiment with the US transducer attached to the right calf, all markers attached, and the treadmill set to 10° incline.

Once the participants were on the treadmill, a static measurement was first made in which they were asked to keep both feet parallel, stand upright and look straight ahead. Next, we recorded the ankle range of motion (ROM), as follows. The participants were asked to stand on one leg, then bend the other at a 90° angle in from of them, and perform five maximal plantar- and dorsiflexions. Subsequently, the lab assistant activated the treadmill. They gradually increased the velocity until the participant signaled. Participants were instructed to choose a moderate walking speed, similar to walking to the supermarket without haste. That should achieve a walking pattern that is as natural as possible. The self-selected speed of the participants ranged from 0.64 to 1.39 m/s (1.07 $\pm$ 0.19 m/s; M $\pm$ SD).

Once the comfortable speed was found, a one-minute warm-up phase without any measurements occurred so the participants could adapt to their regular gait pattern

(a) Frontal view (b) Back view

Figure 3.4: Participant on treadmill, prepared for the experiment.

and get used to walking on a treadmill. Following that, we recorded five to seven walking trials, each lasting around 20 seconds, until the participant had walked for a total accumulated time of approximately three minutes. The treadmill stopped, and the incline changed from 0° (0%) to 10° (17.63%). Subsequently, another static measurement was done. Participants once again walked at the previously chosen speed after a one-minute warm-up. However, this time, approximately two minutes of walking trials were recorded, which was shorter than in the no incline condition, to control effort and avoid fatigue. The treadmill was then returned to its original state. The ultrasound (US) transducer was then switched from the left to the right calf before the protocol was repeated from the beginning.

3.4 Data Processing

After collecting the data from all participants, it is important to filter the required information. Depending on the objective of the analysis, several steps were per-

formed on the kinematic, kinetic and ultrasonic data sets. Each processing step was performed exclusively for the dominant side of the participant in order to maintain a consistent working framework. It was assumed that the dominant side exerts a greater influence on the gait and movement patterns than the non-dominant side.

3.4.1 Ultrasonography

The first step of the data processing was to convert the US image data into a suitable video format to work in the *UltraTrack* software, developed by Lichtwark and Farris[28], which uses the affine flow algorithm described in Section 2.2.2. The .tvd files were changed to the .avi format for that. Subsequently, from the recordings, one trial for the 0° condition and one for the 10° condition were chosen for each participant. Trials were chosen based on the criteria of displaying the most parallel aponeuroses and optimal video contrast. This selected trial subsequently forms the basis for both kinematic and kinetic analyses.

In the following step, the videos was loaded into *UltraTrack*. Since surrounding borders and information about the settings used during the ultrasonography were visible on the raw videos, it was necessary to crop them. That resulted in an image section containing only the biological tissue. A ROI had to be defined after choosing the proper image depth of 50 mm. It was set as the "[...] outline of the cross-section of the muscle of interest [...]" and "include[s] the thick muscle fascia, or aponeurosis, that borders the muscle"[28]. According to Lichtwark and Farris, the fixed ROI is only recommended when there is no movement of the aponeuroses during the video. However, the "fixed ROI" option was not selected because significant movement was visible (compare [28]).

The final step before running the tracking algorithm was the choice of the fascicle. For all three conditions (static, 0° walking, and 10° walking trial), the attempt was made to select the same fascicle make the results comparable.

After running the algorithm, a key-frame correction was applied using the HS of the trials as key-frames. Figure 3.5 compares the changes of the plotted graph of FL. The seen downward trend in Figure 3.5a was corrected so that the FL at HS remained on the same level (compare Figure 3.5b).[1]

The saved data in .txt files were transferred to *Excel* v. 2203 Build 16.0 (*Microsoft*, USA) and analyzed using *Matlab R2019b* v. 9.7.0 (*The MathWorks Inc.*, USA). From the static trials, the mean was calculated. Peak and minimum FL were extracted for each walking trial using the findpeaks-function. From these quantities, the following parameters for each gait cycle in the chosen trials were defined and calculated: the *ultrasound measured fascicle stretch range (USR)*, which represents the total fascicle stretch range, the static to maximum (*USR_MAX*) and static to minimum (*USR_MIN*) range.

3.4.2 Joint Kinematics and Kinetics

In order to obtain kinematic data from the raw material, the recorded trials had to be reconstructed, cut, and labeled. For this, *Nexus* was used again. Static and gait tests were shortened to a few images if they included longer periods without movement. After assigning the appropriate markers to the points according to the GAIT Workflow Sheet in the appendix, gaps were filled using different techniques provided by the software. Gaps can occur when some markers are flickering or hidden by body parts. Finally, non-used markers were deleted from the trial to continue with further processing steps.

Visual 3D v.4.90 (*C-motion Inc.*, USA) was employed for extracting the kinematic and kinetic data. A pipeline written by a colleague in the JWI within this software calculated various variables. The pipeline also applied a bidirectional low-pass

[1] An attempt was made to utilize automated tracking, as described by Cronin[33], but it was ultimately dismissed. Although the results were similar, the significantly increased workload rendered it not cost-effective.

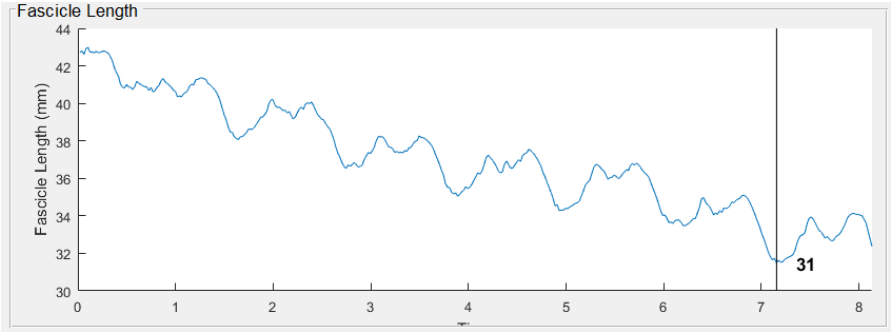

(a) Before key-frame correction

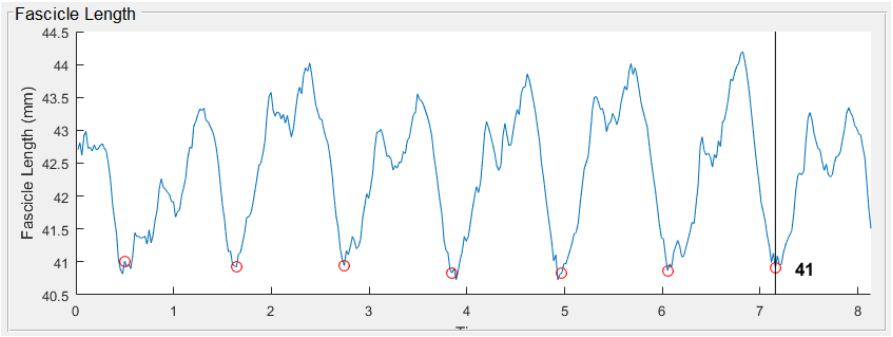

(b) After key-frame correction

Figure 3.5: Graph of fascicle length using key-frame correction in *UltraTrack*.

Butterworth filter with a 10 Hz cut-off frequency to filter the marker trajectories and force plate data. Afterward, joint angles of the ankle, knee, and hip for both sides and all planes (sagittal [x], frontal [y], and transverse [z]) were determined using link-model-based calculations.

Further, net joint moments were calculated with the same model and standard inverse dynamic equations. Lastly, *Visual 3D* normalized these moments and the GRF data to the body mass of the corresponding participant. All processing steps, including filters and calculations, were implemented following recommendations of *C-motion Inc.*

The pipeline ejected much more data than needed with the described steps. For the present work and further analysis, the following dependent parameters of the sagittal plane (x) were selected:

During the whole gait cycle

- ankle angles
- knee angles
- hip angles

During the stance phase

- ankle moments
- knee moments
- hip moments

Via Excel and a visual display, the properly executed step cycle of the previously chosen trial (see Section 3.4.1) was extracted for each participant. These cycles serve as the foundation for the analysis phase. A Matlab script was used to identify maximum and minimum values for the specified framework. From the motion capture data, the following parameters were obtained and used for analysis: angles at heel-strike (initial ankle angle (IAA), initial knee angle (IKA), and initial hip angle (IHA)) and peak extension/flexion moments (maximum plantarflexion moment (MPFM), maximum knee extension moment (MKEM), maximum knee flexion moment (MKFM), maximum hip extension moment (MHEM), maximum hip flexion moment (MHFM)) for each joint. For a more detailed explanation, refer to Table 3.3 and Figure 4.5. Furthermore, the cycles were assembled to represent a mean for each parameter and participant to enable comparison across all participants.

Ultrasound		
	USR	total range of FL (max-min); stretch
	USR_MAX	static to maximum range
	USR_MIN	static to minimum range
Joint angles		
Ankle	*IAA*	initial angle at heel-strike
Knee	*IKA*	initial angle at heel-strike
Hip	*IHA*	initial angle at heel-strike
Joint moments		
Ankle	*MPFM*	maximum plantarflexion moment
Knee	*MKEM*	maximum extension moment
	MKFM	maximum flexion moment
Hip	*MHEM*	maximum extension moment
	MHFM	maximum flexion moment

Table 3.3: Description of ultrasound, kinematic and kinetic parameters later used for statistical analysis. See Figures 4.2 and 4.5 for further indication within the progression plots of the fascicle length (FL), angles and, moments.

3.5 Statistical Analysis

All statistical analyses were conducted using *IBM SPSS Statistics* version 28, USA. Given that each participant underwent repeated measurements for two conditions (0° and 10° incline), two-sided paired t-tests for cases with assumed parametric distributions and Wilcoxon signed-rank tests for non-parametric distributions were employed. The significance level (α) was set at 0.05 for each test to ensure a reliable and consistent data evaluation.

Before conducting the t-tests or Wilcoxon signed-rank tests, the normality of the data was checked using the Shapiro-Wilk test. This method, suitable for small sample sizes in this study ($N < 50$), enabled an accurate assessment of distribution characteristics. In accordance with this test, the null hypothesis (H_0) assumed a normal data distribution, serving as a critical initial step in the statistical analyses. To enhance the interpretability of the results and gain deeper insights into the prac-

tical significance of the observed differences, effect size tests were also conducted. Given the limited sample sizes for each condition and parameter, the Hedges' g test was chosen, as it is well-suited for situations with small sample sizes. Using Hedges' g allowed to quantify the effect sizes and understand the magnitude of differences between the conditions. Effect sizes below 0.5 indicated a small effect, suggesting that the observed differences had a relatively modest impact. If the effect sizes fell within the range of 0.5 to 0.8, it was categorized as a medium effect, signifying a more moderate and noteworthy influence. A large effect was evident for cases where the effect size exceeded 0.8 ($g > 0.8$), highlighting significant disparities between the conditions.

Given that other studies did not specifically explore differences among participants, as is the focus of this work, an additional objective was to compute mean results for all participants as a collective population. This approach aimed to enhance understanding and categorization of the results. The average values of the participants were calculated and used for the subsequent evaluations. The paired t-test was used again, as the design within the participants remained unchanged. The significance level and the other methods also stayed identical. Conditions would not exhibit any differences in the mean values if the determined p-value was above .05.

The master's thesis extensively employed correlation tests for deeper insights and rigorous analysis. That examines the relationships between the described variables. The goal was to investigate whether changes in one variable are associated with changes in another variable and to assess the extent of this relationship. To ensure the validity of the findings, appropriate statistical methods were selected based on the nature of the parameters under investigation.

The Pearson's R correlation coefficient was relied upon for variables exhibiting a normal distribution. This classic method facilitated the quantification of the

linear relationship between normally distributed variables, providing insights into potential patterns and dependencies.

However, the importance of addressing non-normally distributed variables was acknowledged. Spearman's rank correlation coefficient was employed for these cases, representing a robust non-parametric measure. Spearman's ρ effectively captures monotonic associations between variables, enabling exploration and discovery of potential links that might not be evident through Pearson's R. For both approaches, results with a p-value below .05 are considered correlated.

CHAPTER 4

Results

The conducted study aimed to collect kinematic and kinetic data concerning the ankle, knee, and hip, along with capturing movement and changes in the musculus gastrocnemius medialis. Utilizing a motion capture system and an ultrasound device, comprehensive data were recorded under two different gradient conditions. Subsequent post-processing enabled the extraction of respective angles and moments of the joints, as well as the change in length of the muscle, from the raw data. The subsequent chapter presents and partially compares these results. However, due to inconsistencies in the collected data from the US device and certain participants, concerns emerged regarding the reliability of the data or the accuracy of the measurement procedure. A more comprehensive analysis of the underlying errors is provided in Chapter 5.

4.1 Final Sample

The next two sections outline the reasons behind the exclusion of certain parameters and participants from further data analysis. Additionally, they provide the final

demographic data of the participants whose data is included in the study.

4.1.1 Excluded Data

The analysis of the parameters *USR_MAX* and *USR_MIN* had to be omitted. During data processing, it became evident that the mean values for static recordings consistently exceeded those of the corresponding walking recordings, leading to both *USR_MIN* and *USR_MAX* consistently producing negative values. The initial expectation was for the means to be closer to those observed during walking, making them comparable.

To ensure the validity and credibility of the study's conclusions, only twelve of the 15 participants were included in the final sample. This decision was prompted by irregularities in the data set that were detected during processing. In particular, the motion capture data contained errors that could not be corrected even after reprocessing. In some cases, angles and moments were not recorded during the entire gait cycle, which made it impossible to evaluate the selected parameters. Consequently, participants 9 and 13 were excluded from the study after careful evaluation.

Furthermore, Participant 3 showed an unusual progression of the knee and hip joint moments compared to the mean of all others as well as the graphs in the reviewed literature (see Figures 2.4 and 4.1). After thorough testing, consultation with colleagues, and conducting a fresh analysis, the presumed error in the data has not been discovered.

Examining the knee joint moment's progression, as depicted in Figure 4.1a, has highlighted some observations. An inexplicable absence of the extension moment was identified, coupled with a confounding three-fold increase in the flexion moment when walking on an inclined surface. At first glance, the graph of Participant 3 appears to be shifted in the direction of flexion. However, despite this apparent

shift, it is important to recognize that the integrity of the data regarding the start and end points has been verified and found to be correct. A definitive confirmation of a shift based on these observations alone is impossible.

An examination of the hip joint moment's progression, as illustrated in Figure 4.1b, reveals even more pronounced discrepancies between Participant 3 and the rest of the participants. The maximum extension moment *MHEM* is four times higher in 0° and 10° inclined conditions. While some literature reports moments reaching almost 2 $\frac{Nm}{kg}$ during inclined walking conditions [25], and others confirm values of approximately 1.7 $\frac{Nm}{kg}$ [20], it is essential to acknowledge that none of the existing literature supports an extension moment as high as observed in Participant 3 during level walking conditions.

Given the uniqueness of this divergent progression in only one participant, it raises concerns regarding data accuracy and potential errors. The magnitude of the observed hip joint moment for Participant 3 seems unreasonably high compared to the rest of the participants, who did not exceed 1 $\frac{Nm}{kg}$.

Even though ankle angles and moments, as well as the knee and hip angles of Participant 3, follow the appropriate similar progression of all other participants, the mismatch in knee and hip moments challenges the validity of the data. Consequently, Participant 3 was also excluded from further data analysis.

4.1.2 Participants

	Age (years)	Stature (cm)	Weight (kg)
Mean	31.3	178.88	72.27
SD	4.48	10.06	11.61

Table 4.1: Anthropometric data for participants included in the data analysis

After excluding of three participants for the above described reasons, twelve

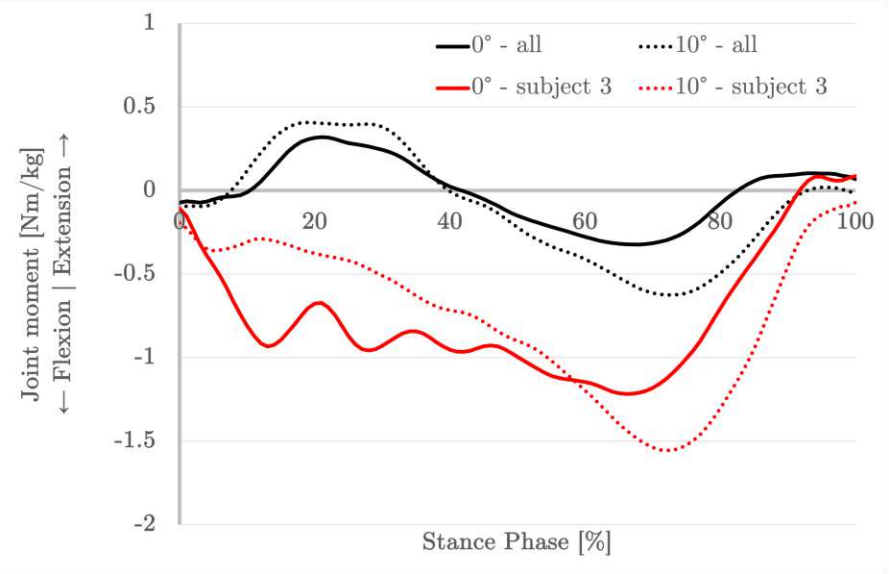

(a) Knee Moments

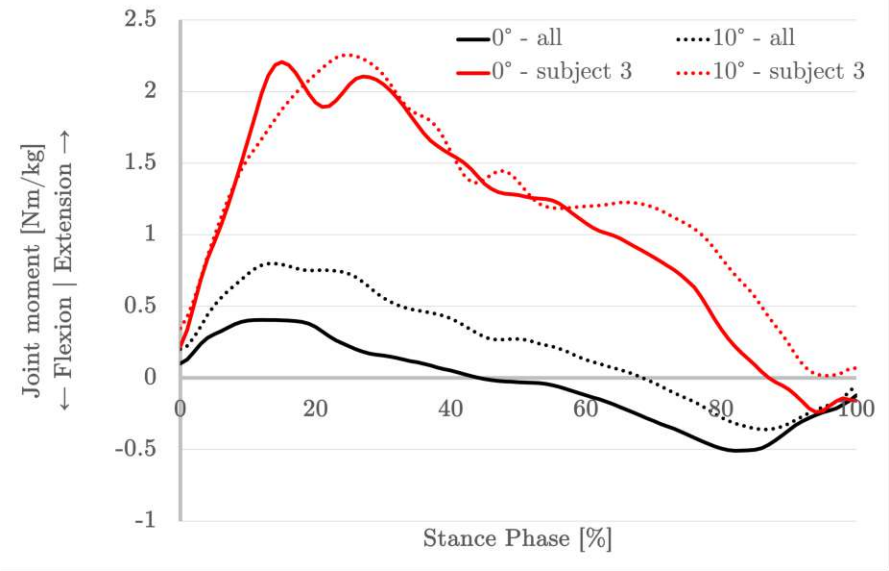

(b) Hip Moments

Figure 4.1: Comparison of the progression of knee and hip joint moments between Participant 3 and the rest of the participants. The solid line indicates the 0° condition, while the dotted line represents the inclined walking. The red lines are referenced to Participant 3, whereas the black ones represent the mean of all other participants.

participants (age: 31 ± 4.5 yr, height: 178.9 ± 10 cm, body mass: 72.3 ± 11.6 kg; M ± SD, see Table 4.1) are included in further data analysis. These healthy male subjects constitute the statistical sample for the study.

4.2 Testing Data for Normality

The normality of distributions within each participant for all outlined parameters was examined. The results of these tests showed no significant deviations from normality, which provides a sound basis for assuming a normal distribution for each participant and each parameter, thus confirming the use of t-tests in these cases. However, when collecting the parameters across multiple participants, the results differed. The Shapiro-Wilk test conducted on the assembled data showed significant deviations from normality in *MKFM* at a 10° slope ($W(n = 12) = .766$, $p = .004$). These findings necessitate the consideration of an alternative distribution model and, consequently, statistical tests for this particular case.

4.3 Ultrasound Data

A general decrease in FL was found during incline compared to level walking for all participants. Thus, when walking on an incline, the measured persons' gastrocnemius medialis stretched less. While the minimum length decreased from an average of 44.5±5.0 mm to 40.8±7.7 mm ($t(11) = 2.046$, $p = .033$, $g = .549$), peak values changed from 48.4±4.7 to 46.6±8.4 mm (no significance: $t(11) = 0.841$, $p = .209$, $g = .226$). The *USR* for all participants during incline compared to level walking increased from 4.0 mm to 5.7 mm ($t = -3.012$, $p = .012$, $g = -.809$). Figure 4.2 shows a representative progression of the fascicle length of a participant during one walking trial. The solid line represents walking on level ground, while

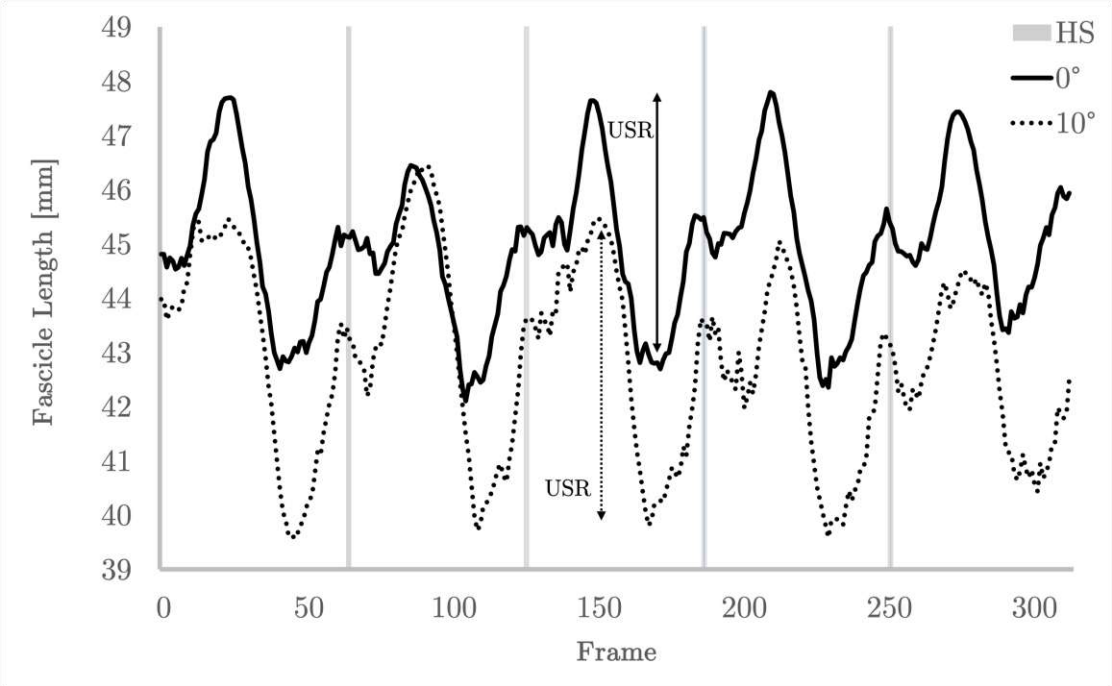

Figure 4.2: Progression plot of the fascicle length (FL) per frame during an entire walking trial of one representative participant. The solid line indicates the 0° condition, while the dotted line represents the inclined walking. The vertical gray lines mark the heel-strike (HS). Ultrasound measured fascicle stretch range (*USR*) calculation is shown for both settings.

the dotted line symbolizes walking on a 10° incline. The trial starts with a HS and ends just before the sixth one. All strikes in between are marked with a gray line. Additionally, the parameter of interest *USR* was plotted on the graph for the 0° and 10° conditions, respectively. A more detailed section in Figure 4.3 plots the mean fascicle length over one gait cycle. When walking without incline, the fascicle length remains at a similar level until it increases after about 20% of a gait cycle, during mid stance. It peaks at around 47.5 mm in length during the terminal stance phase. The minimum value of 43 mm is reached between 65% and 78% of the gait cycle, partly representing the initial and mid-swing phases. During inclined walking, the progression looks similar, but the values show a smaller magnitude.

The cycle starts at 44 mm FL, which remains until the start of the mid-stance at 12%. This is slightly earlier compared to level ground walking. The peak, however, is reached around the same time, attaining 45.5 mm. Also, the subsequent slope of decrease and timing of the minimum value are similar in both conditions. When walking on a 10° incline, the minimal value of the FL is about 40 mm.

Figure 4.4 shows the comparison of *USR* between the conditions for each par-

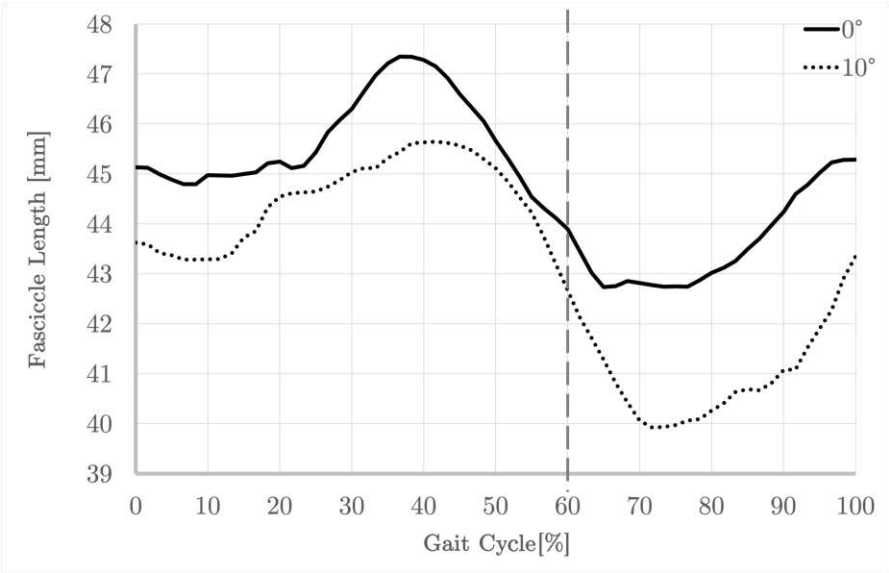

Figure 4.3: Mean progression plot of the fascicle length (FL) for a separate gait cycle in percent [%] of one representative participant. The solid line indicates the 0° condition, while the dotted line represents the inclined walking. The dashed vertical line marks the transition from the stance to the swing phase.

ticipant. The black box plots represent the values for non-inclined, and the gray ones for 10° inclined walking. For nearly all participant, the mean of the inclined setting is higher than the one of level walking. Only for Participant 5, it appears vice versa. Eight participants showed a significant effect during incline walking. Looking at the plot, one can notice that the differences between 0° and 10° are immense for a few participants. Some differences do not even amount to 1 mm, while others reach several millimeters. The most noteworthy discrepancy can be

seen in Participant 7. Here, the elongation differs from walking on level ground to walking uphill by about 6 mm.

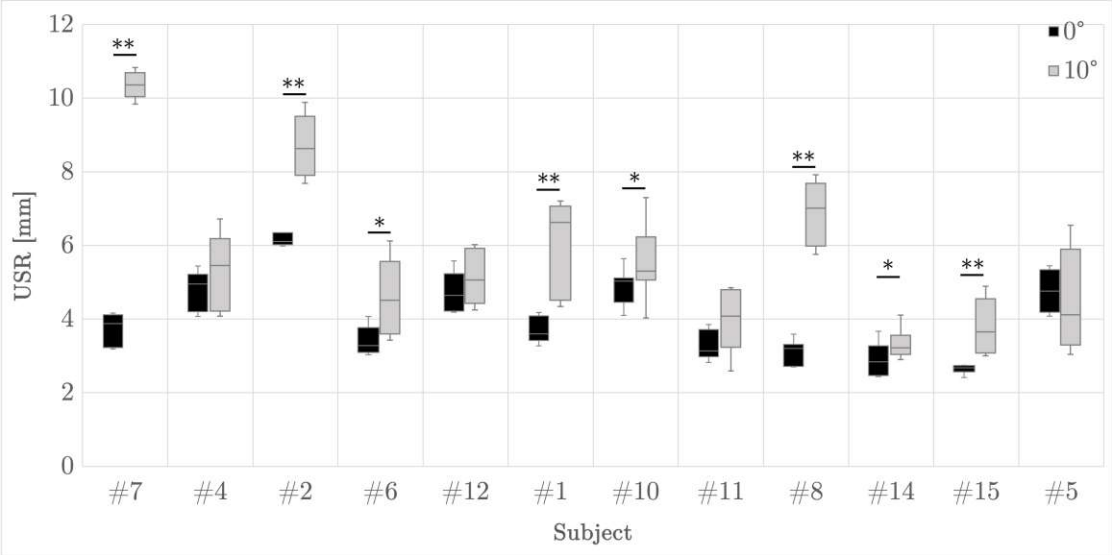

Figure 4.4: Box plots of the ultrasound measured fascicle stretch range (*USR*) data sorted from lowest to highest walking speed. Black boxes show values for non-inclined walking and gray boxes for the 10° inclined condition. For each pair $*$ indicates a p-value $< .05$, $**$ signifies $p < .01$.

Participant			#7	#4	#2	#6	#12	#1	#10	#11	#8	#14	#15	#5
US	**USR**	p	.00**	.20	.00**	.02*	.17	.01**	.03*	.07	.00**	.02*	.00**	.31
		eff.	↑L	↑S	↑L	↑L	↑S	↑L	↑L	↑M	↑L	↑L	↑L	↓S

Table 4.2: Calculated p-values for paired t-tests and the according effect sizes after Hedges' g for the ultrasound data; S = small effect ($|g| < 0.5$), M = medium effect ($0.5 \leq |g| \leq 0.8$), L = large effect ($|g| > 0.8$). The columns represent the participants included in the calculations. * indicates a p-value $< .05$, ** signifies $p < .01$. Participants 4, 5, 11, and 12 are marked, since no sign. was found for ultrasound measured fascicle stretch range (*USR*). ↑: increase, ↓: decrease of the parameter.

No significant difference in the fascicle stretch range was observed for the remaining four participants. For Participant 4, the *USR* during 0° and 10° conditions did not

differ, $t(4) = -0.93$, $p = .2$. The same observation was made for 5 ($t(6) = 0.53$, $p = .31$), 11 ($t(5) = -1.78$, $p = .07$) and 12 ($t(6) = -1.03$, $p = .17$). However, these results show only small (4, 5, 12) or medium (11) Hedges' effect sizes. In contrast, the calculated effect size of the aforementioned data is > 0.8 (compare Table 4.2).

4.4 Joint Kinematics and Kinetics

The left side of Figure 4.5 visualizes the progression of the ankle, knee, and hip angles in degrees (°) for an entire gait cycle. The graphs are a result of averaging the extracted cycles of all participants. Like in Figure 4.2 or 4.3, the solid line represents the 0° incline walking, and the dotted one depicts the 10° condition. The vertical dashed gray line marks the transition from the stance phase (0-60% of the gait cycle) to the swing phase (60-100%). The parameters *IAA* to *MHFM* are added to the graphs of the respective joints to show where they were extracted from. Furthermore, it is visible how the timings of peak and minimum values change partly.

Looking at the plots of the angles, one can see the graphs of the inclined walking start with a higher value for all joints. The ankle graph increases afterward and stays on a plateau of dorsiflexion for around 15% of the whole cycle. The following decrease results in the minimum plantarflexion, similar to the value of the 0°-graph. Also, the decrease moved parallel in both conditions. In contrast to level walking, rises the 10°-graph to a higher level during the swing phase, reaching a local dorsiflexion peak just before the next HS.

The knee graphs of both conditions look very similar. Even though the dotted graph starts on a higher value of *IKA*, the global mini- and maximum magnitudes stay on the same level as the solid one. In the graph representing the 10° incline

walking, the first slope from flexion to extension is steeper, and for the 0° incline condition, it is the second slope.

As with the knee graph, the two curves in the hip graph look very similar. The solid line is flatter than the dotted one. Thus, the beginning value of *IHA* and the flexion peak at the end of the gait cycle are higher. However, the minimum extension of the hip does not seem to differ. The timings of when the mini- and maximum emerge appear equal, too.

The right side of Figure 4.5 shows the progression of the joint moments during the stance phase. Again, all extracted parameters are drawn in, and the solid and dotted lines represent the 0° and 10° incline conditions, respectively. Based on the extrapolation to 100%, the phases are divided into the following sections: 0-5% HS; 5-20% loading response, 20-52% mid stance, 52-83% terminal stance, and 83-100% pre-swing.

The first plot shows how the progress of the ankle joint moments change. First, a dorsiflexion moment is induced in the joint during physiological gait on a level surface. However, when walking on a 10° inclined treadmill, almost no moment of dorsiflexion occurs at all. The growth that follows the HS or loading response is almost parallel in the two states. The participants tended to produce a higher plantarflexion moment during inclined walking, while the subsequent drop looks similar in both walking conditions.

Both graphs for the knee joint moment have a parallel course. The maximum extension moment *MKEM* is at the same level and occurs at a similar time. The latter also applies to the peak moment of flexion. However, the value here is relatively lower when walking on level ground than on an incline. In contrast to the 0°-graph, no further extension moment can be seen in the 10° chart.

The last tile at the bottom right, on which the hip joint moments are plotted, shows the greatest visual discrepancy. Even though both graphs show increase

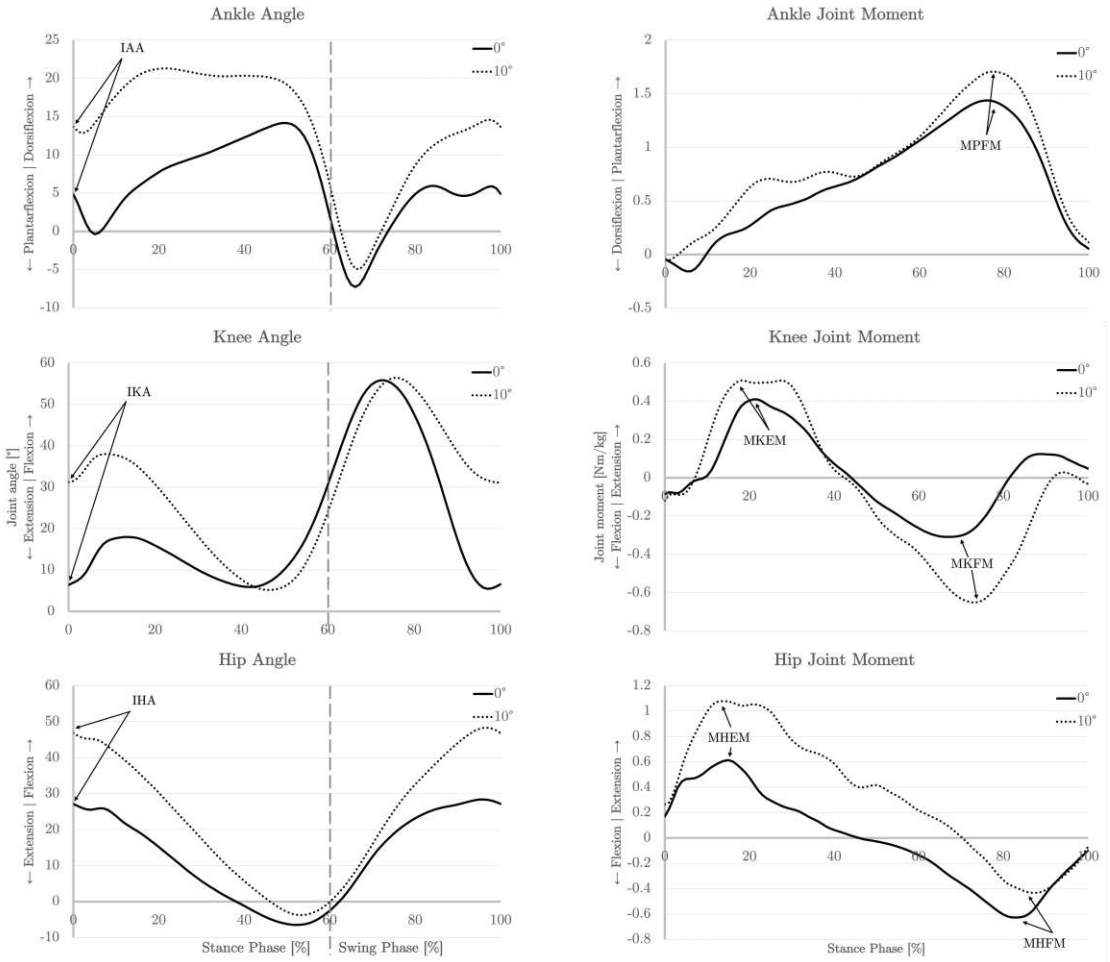

Figure 4.5: Angle and joint moment data for ankle, knee, and hip. Angles are plotted against the full gait cycle (transition from the stance to the swing phase marked by the vertical dashed line), and moments against the stance phase are normalized to 100%. The corresponding extracted parameters (initial angle angle (*IAA*), initial knee angle (*IKA*), initial hip angle (*IHA*) and maximum plantarflexion moment (*MPFM*), maximum knee extension moment (*MKEM*), maximum knee flexion moment (*MKFM*), maximum hip extension moment (*MHEM*), maximum hip flexion moment (*MHFM*)) are drawn into the plots.

initially, the peak extension moment of the hip *MHEM* is much higher during 10° walking and rises to 1.25 $\frac{Nm}{kg}$, thus doubling the value of *MHEM* for level walking. Both graphs decrease parallel to each other, resulting in a minimum joint moment (*MHFM*) almost simultaneously during the terminal stance. At this point of the

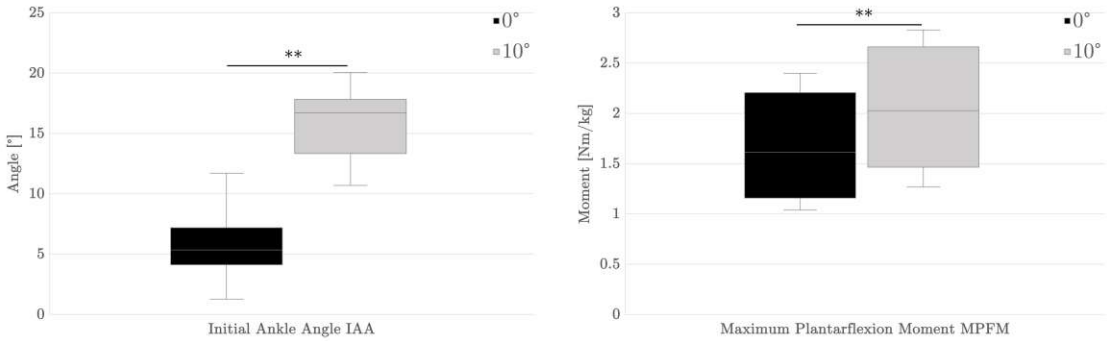

(a) Ankle angle parameters (b) Ankle moment parameters

Figure 4.6: Comparison of the ankle parameters for all participants' means. For each pair $*$ indicates a p-value $< .05$, $**$ signifies $p < .01$.

maximum flexion moment, the 0° diagram has a higher value than that of 10°.

Table 4.3 provides a summary of the t-test results between the walking conditions for each parameter, including the p-values and Hedges' g values. When comparing the two conditions of all participants, significant differences were found for the parameter *IAA* of the ankle angle ($t(11) = -13.295$, $p =< .001$, $g = -3.569$). The parameter increased significantly when the participants walked on an inclined surface. The corresponding box plot can be seen in Figure 4.6a. There is a pretty visible difference between *IAA* as the graph in Figure 4.5 suggested.

Assumptions of a statistical change of the *MPFM* have also were confirmed. The mean significantly increases from around 1.69 $\frac{Nm}{kg}$ to 2.04 $\frac{Nm}{kg}$ ($t(11) = -12.007$, $p =< .001$, $g = -3.223$), which effectively depicts an increase in plantarflexion moments of the ankle during walking uphill. In comparison with the *IAA*, the values of the *MPFM* vary more between the participants, as seen in Figure 4.6b.

The analysis of the angle parameter of the knee *IKA* reveals similar results to *IAA*. Its mean advances immensely for the population with an increasing incline from 8.1° to 36.6° (refer to Figure 4.7a). This outcome has shown to be statistically significant with $t = -19.561$, $p =< .001$, and a large effect size via Hedges' correction ($g = -5.251$).

		0°	10°	p	g
USR	[mm]	4.0	5.7	.012*	−0.809
IAA	[°]	5.7	15.9	< .001**	−3.569
IKA	[°]	8.1	36.6	< .001**	−5.251
IHA	[°]	31.7	55.6	< .001**	−8.566
MPFM	$[\frac{Nm}{kg}]$	1.69	2.04	< .001**	−3.223
MKEM	$[\frac{Nm}{kg}]$	0.65	0.75	.176	−0.389
MKFM	$[\frac{Nm}{kg}]$	−0.35[1]	−0.83	.002**	1.164
MHEM	$[\frac{Nm}{kg}]$	0.77	1.47	.002**	−1.121
MHFM	$[\frac{Nm}{kg}]$	−0.86	−0.62	.058	−0.569

Table 4.3: Mean values and results of the t-tests for the comparison of parameters between 0° and 10° incline. For each pair $*$ indicates a p-value $< .05$, $**$ signifies $p < .01$. [1]Calculated with Wilcoxon signed-rank test.

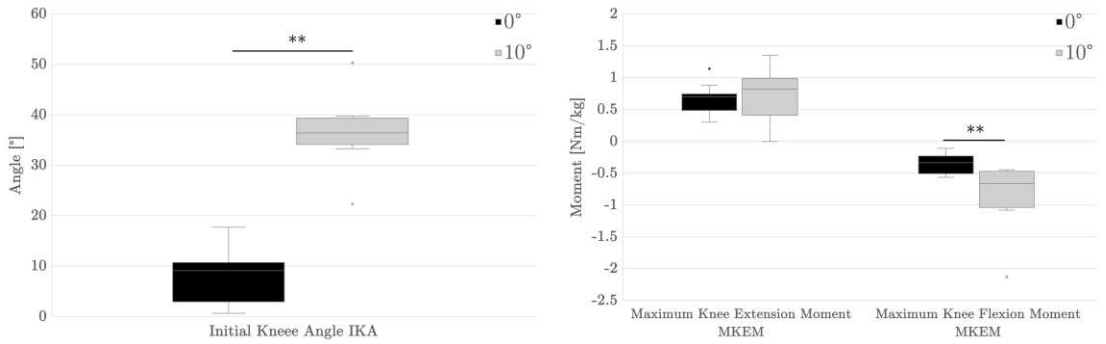

(a) Knee angle parameters

(b) Knee moment parameters

Figure 4.7: Comparison of the knee parameters for all participants' means. For each pair $*$ indicates a p-value $< .05$, $**$ signifies $p < .01$.

Even though a change of the *MKEM* is visible in Figure 4.5 tile four, and is also displayed in Figure 4.7b, no significance has been verified ($t(11) = -1.448$, $p = 0.176$, $g = -0.389$). The analysis reveals a significant trend in the maximum knee flexion moment (*MKFM*) as the incline angle changes. Specifically, there is a considerable reduction in the knee flexion moment when transitioning from level walking to a 10° incline. The mean flexion moment of the knee demonstrates a substantial decrease, almost doubling the initial value, from approximately -0.35

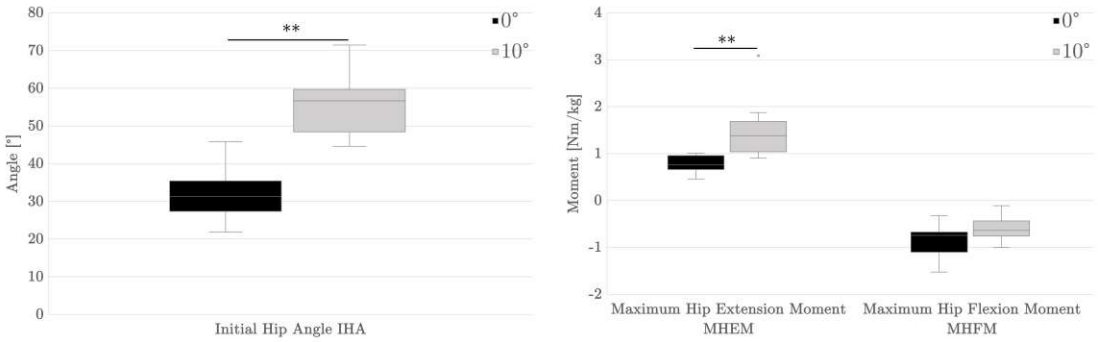

(a) Hip angle parameters (b) Hip moment parameters

Figure 4.8: Comparison of the hip parameters for all participants' means. For each pair $*$ indicates a p-value $< .05$, $**$ signifies $p < .01$.

$\frac{Nm}{kg}$ to -0.83 $\frac{Nm}{kg}$ ($Z = -3.059$, $p = .002$).

Precise calculations have confirmed the noticeable and distinct disparity in the initial hip angle, as depicted in Figure 4.5 and Figure 4.8a. The initial hip angle (*IHA*) exhibits a significant increase, rising from 31.7° to 55.6° ($t(11) = -31.909$, $p < .001$, $g = -8.566$).

Furthermore, the maximum hip extension moment (*MHEM*) displays a notable increase during inclined walking compared to level walking, reaching statistical significance as it elevates from 0.77 $\frac{Nm}{kg}$ to 1.47 $\frac{Nm}{kg}$ ($t(11) = -4.176$, $p = 0.002$). This large effect size of $g = -1.121$ emphasizes the substantial impact of this change across the entire participant population.

Interestingly, no statistically significant mean difference was observed when comparing walking on level ground to walking on a 10° incline regarding the *MHFM*. Although the value changed from -0.86 $\frac{Nm}{kg}$ to -0.62 $\frac{Nm}{kg}$, the difference did not reach statistical significance ($t(11) = -2.118$, $p = .058$, $g = -.569$). Both box plots of the hip moment parameters are displayed in Figure 4.8b.

4.5 Correlation

In order to examine the potential relationships between the initial ankle angle *IAA* and the rest of the defined parameters, correlation analyses were conducted. Table 4.4 provides a comprehensive summary of the outcomes. Significant correlations were observed in only three instances.

Only the *IAA* and *MHEM* show a considerable relationship during level walking ($R = .526$, $n = 12$, $p = .039$). As participants walk on a 10° incline, a statistically significant negative correlation emerges between the *IAA* and *USR* ($R = -.564$, $n = 12$, $p = .028$). This prominent correlation suggests a connection between those two variables, revealing their interdependence during inclined walking.

Moreover, the correlation analysis displays a significant relationship between the *IAA* and the *IKA* during inclined walking. This correlation, with a coefficient of $R = .592$ ($n = 12$, $p = .021$), highlights a potential relation between the angles of the ankle and knee joints. This finding points toward a possible link between the movement patterns of these two joints during walking on the induced slope.

Figure 4.9 displays two scatter plots that compare the value pairs of *IAA* and *USR*.

	0°		10°	
	Correlation	p	Correlation	p
USR	.264	.204	−.564*	.028
IKA	.246	.221	.592*	.021
IHA	.145	.327	−.107	.370
MPFM	−.193	.274	−.128	.346
MKEM	.127	.347	−.137	.336
MKFM	−.148	.323	−.084[2]	.398
MHEM	.526*	.039	.155	.315
MHFM	−.228	.238	−.219	.247

Table 4.4: Calculated correlation coefficients and p-values of the ultrasound, angle, and moment parameters in relationship to initial ankle angle (*IAA*). [2]The correlation coefficient is Spearman's ρ here.

The diagram on the left side (Figure 4.9a) illustrates the results obtained during level walking. Conversely, Figure 4.9b depicts the same comparison during the 10° incline walking condition. Similar to the subsequent plots, the x-axis of the left plot, which always features *IAA*, spans from 0° to 12°. Conversely, the x-axis of the right plot, corresponding to the 10° incline condition, ranges from 10° to 22°. The y-axis of the *USR* plots here has a range of 10 mm for both conditions.

A tendency towards a positive correlation with a flat slope is observed while walking on level ground. However, this correlation shifts to a confirmed negative pattern when walking uphill. While there seemed to be an increase in *USR* values with the elevation of *IAA* during level walking, it's crucial to highlight that these changes did not reach statistical significance in the conducted analysis. In contrast, a 10° incline condition resulted in a significant decrease in *USR* values with increasing *IAA*.

Figure 4.9a suggests the possibility of a correlation, which is supported by the relatively low dispersion of data points. In particular, the single data point positioned at the upper edge, where *USR* is approximately 6.5 mm and *IAA* is around 5°, stands out from the rest of the data. In contrast to picture 4.9b, several data points are on the trend line.

The direction of correlation for the value pairs of *IAA* and *IKA*, as illustrated in Figures 4.10a and 4.10b, remains consistent. Despite the lack of statistical significance for the level walking condition ($R = .246$, $p = .221$), the trajectory of the trend line suggests a positive slope, implying a potential positive correlation. However, the dispersion of data points is noticeably wide, aligning the visual impression with the calculated coefficient that a meaningful correlation is lacking. During inclined walking, it is worth noting that two data points stand out visually and appear to deviate from the expected pattern. One data point corresponds to an *IKA* of approximately 20° and the other at around 50°. The remaining pairs

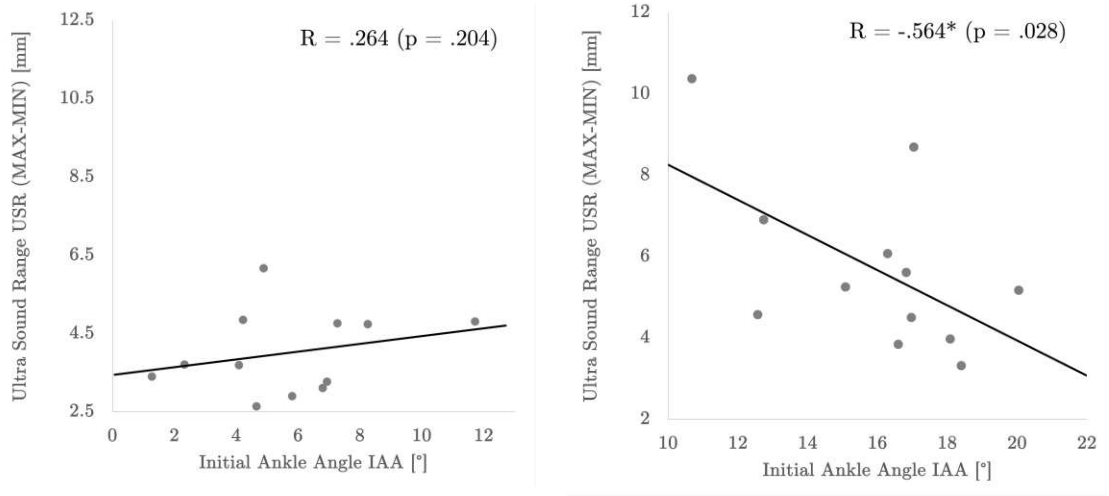

(a) 0° incline

(b) 10° incline

Figure 4.9: Scatter plots of the initial angle angle (IAA) against the ultrasound measured fascicle stretch range (USR) during walking with 0° (left) and 10° (right) inclination, with the line representing the linear trend for each pair of parameters. The Pearson R in the upper right corner indicates the degree of correlation in the data.

are relatively clustered around the rather steep trend line. The highest correlation coefficient R and the smallest p for that condition were computed.

The last pair of data displayed is *IAA* and *MHEM* (refer to Figure 4.11). The trend lines of both walking situations have a comparable progression, but the plots differ highly in the extent of data point scatter, even though the y-axis range stays the same with 1.5 $\frac{Nm}{kg}$. During level walking, the data points tightly cluster around the best-fit line, whereas in the other walking conditions, the points scatter widely throughout the graph. This observation aligns with the analytical outcomes, with a correlation coefficient of $R = .155$ and a corresponding $p = .315$.

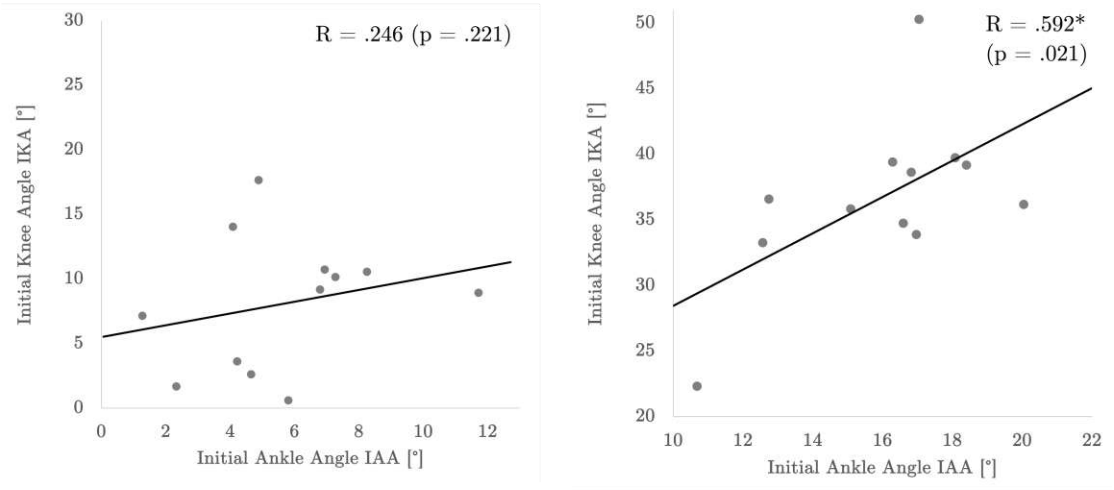

(a) 0° incline

(b) 10° incline

Figure 4.10: Scatter plots of the initial ankle angle (*IAA*) vs the initial knee angle (*IKA*) during walking with 0° (left) and 10° (right) inclination, with the line representing the linear trend for each pair of parameters. The Pearson R in the upper right corner indicates the degree of correlation in the data.

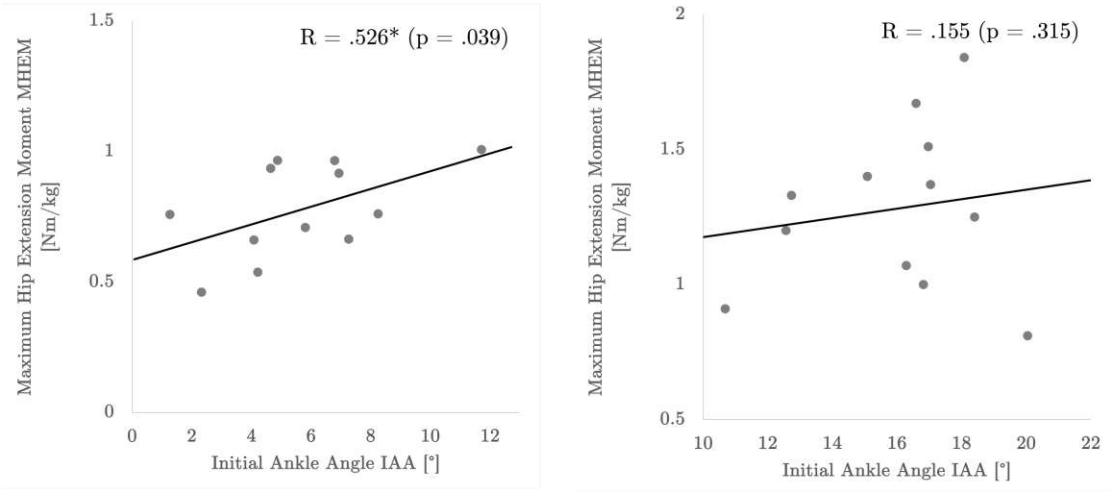

(a) 0° incline

(b) 10° incline

Figure 4.11: Scatter plots of the initial ankle angle (*IAA*) against the maximum hip extension moment (*MHEM*) during walking with 0° (left) and 10° (right) inclination, with the line representing the linear trend for each pair of parameters. The Pearson R in the upper right corner indicates the degree of correlation in the data.

CHAPTER 5

Discussion

The primary objective of this study was to understand the relationship between the gastrocnemius medialis muscle fascicle length and the joint kinematics and kinetics of the lower limbs during walking on an inclined surface. Several findings of the study affirm the hypothesis that a close interaction occurs between muscle and joints. Since this interaction varies among individuals, it proved difficult to identify clear patterns within specific groups of participants. Using correlation calculations, transparent relationships between the initial ankle angle and the knee joint angle, the hip joint angle and the changes in fascicle length were demonstrated. Some of these findings align with results from previous research, as discussed in the sections 5.1 and 5.2. Other outcomes allowed it to analyze the previously mentioned relationships between joints and muscles more comprehensively, for example with a correlation analysis as described in 5.3.

5.1 Kinematics and Kinetics of the Joints

The outcomes regarding the progression of joint angles and moments during level walking are similar to those documented in the cited literature in Chapter 2. When examining Figures 2.3, 2.4, and 4.5, similarities in observed patterns, trends, and peaks become apparent. Figure 5.1 directly compares the angles, while Figure 5.2 contrasts the literature's moment values with those obtained in the study. The notable absence of a clear plantar reflection at HS is a significant deviation that sets the findings apart from others. However, it is worth noting that this particular aspect was also not measured by McIntosh et al.[20]. Factors such as walking speed, foot strike pattern, or conscious adjustments to the measurement environment (e.g., walking on a treadmill vs. walking on the ground) might have influenced the observed joint angles. Thus, the validity of the control group characterized by "walking without incline" is approved.

On the other hand, the patterns and values that emerge when walking at an angle

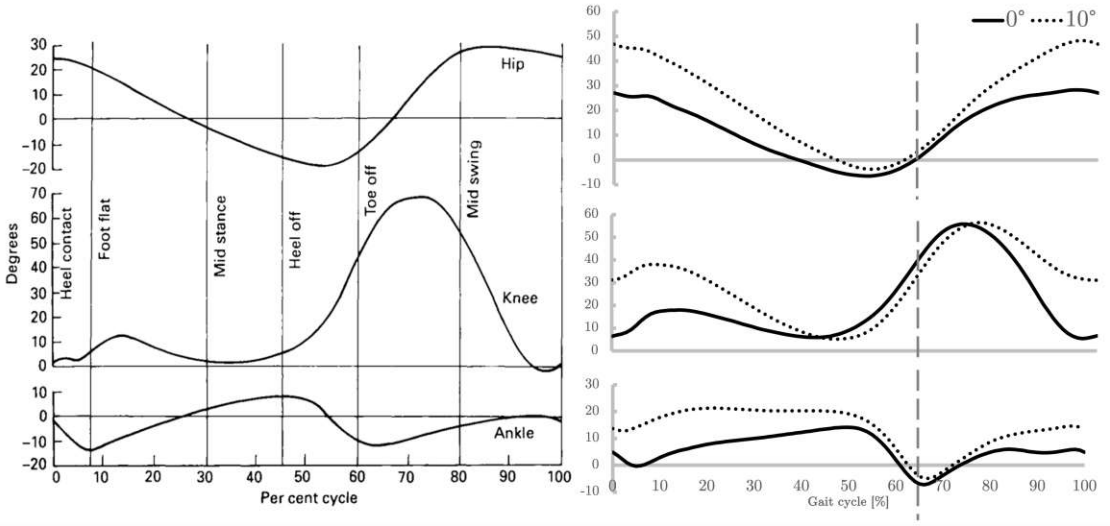

Figure 5.1: Comparison of the lower body joint angle progressions between the literature (left) and the study results (right).

instead of walking on a flat surface show interesting results, some of which differ

from the results of other studies. As expected, there was a significant increase in all angles (*IAA*, *IKA*, *IHA*) at the moment of initial contact, when comparing inclined walking to walking on a level surface for every participant. Walking on an inclined surface means the general posture must be adapted. Ankles are more dorsiflexed to place the foot on the ascending floor, while the knee and the hip need to compensate with flexion to keep an upright standing. These consequences are outlined in studies by Lay et al.[25], McIntosh et al.[20], and Haggerty et al.[21]. Similar progression plots can be found in the respective studies. For McIntosh et al., however, the angles start and end at a 10° higher value during incline walking, which is considerable within the given context[20].

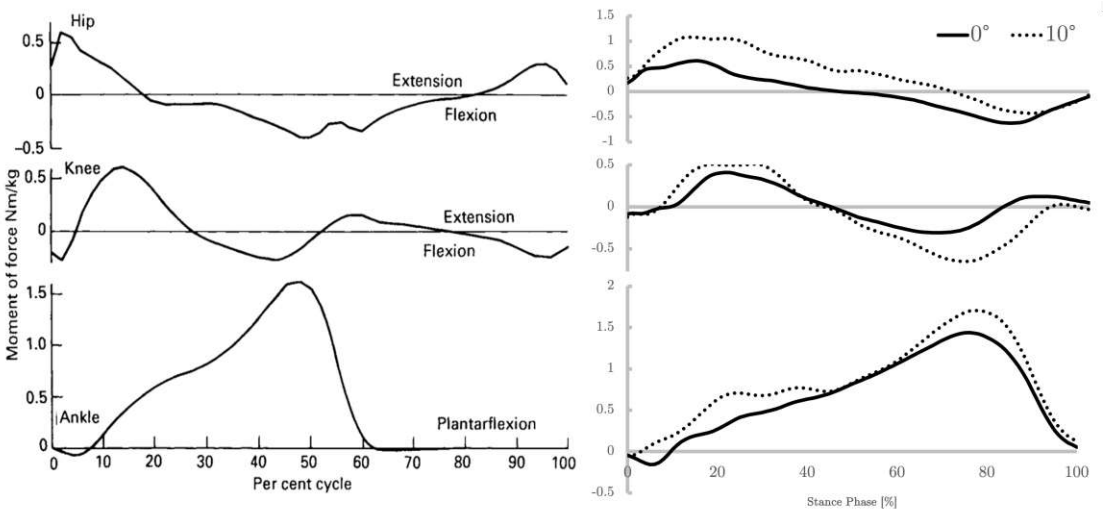

Figure 5.2: Comparison of the lower body joint moment progressions between the literature (left) and the study results (right).

Comparing the moment progression for the two running conditions (solid line for 0° and dashed line for 10°) on the right side of Figure 4.5, reveals numerous similarities, including a parallel slope and the simultaneous occurrence of the MPFM. However, there is a distinct deviation in the ankle moment graph. During the IC of level walking, dorsiflexors typically engage eccentrically to elevate the toes.

Brockett and Chapman attribute this mechanism to factors such as step control and preventing sudden foot drops[64]. Interestingly, this initial dorsiflexion moment was not evident during inclined walking (seen in the upper right graph of Figure 4.5). This divergence implies that the participants did not require this specific mechanism in the inclined condition. The incline contributes to a more dorsiflexed ankle position during the HS phase. Consequently, the foot makes contact with the ground more quickly. It is plausible that this altered ankle positioning reduces the need for significant effort in controlling the foot position during HS. The need for active control appears to be reduced since the foot is already closer to the ground due to the inclination. This adaptive response could explain the absence of the initial dorsiflexion moment during inclined walking, as observed in the data.

In the late stance phase, an increase in *MPFM* and an increase in *MKFM* were noted. Remarkably, there was no significant reduction in the absolute value of *MHFM*, as detailed in Table 4.3. While all of the previously mentioned studies confirm the first two results, McIntosh et al.[20] report a significant decrease in hip moments in their study. During uphill walking, the plantar flexors at the ankle need to exert more effort to generate the necessary propulsive force for lifting the body against gravity. This increased force results in a higher plantar flexion moment at the ankle and is necessary to push the body forward and upwards. Additionally, more knee flexion is required to lift the foot off the ground and adapt to the changing terrain. When the foot moves uphill in the swing phase, the knee must be bent more to achieve an appropriate distance from the ground. Furthermore, the knee can be bent further in the stance phase to adapt to the sloping surface. In this study participants kept the hip extension moment relatively stable during uphill walking. This could be attributed to the individuals maintained a relatively upright posture. However, if there are changes in the walking mechanics or the incline is particularly steep, some hip extension adjustments might be needed to

help propulsion and stability, as McIntosh et al.[20] investigated.

A tremendous effort from the hip extensor muscles is required in an early stance. These muscles are responsible for extending the hip joint, propelling the body forward against gravity, and helping to maintain balance. During inclined walking, this demand increases. If it is assumed that as the incline increases, more of these muscles are engaged to provide the necessary force for the incline, it could lead to an increased hip extension moment, as demonstrated in this study. Similar findings have been reported in studies by Lay et al.[25, 27] or McIntosh[20] under various incline conditions, though not consistent with the results of Haggerty et al.[21]. While it was discovered that the hip extension moment increased, no such change could be detected for the knee extension moment. That might occur to ensure optimal and efficient function of the knee joint. The body may prioritize maintaining a constant knee extension moment to avoid overloading the knee joint to guarantee the joint functions optimally and efficiently when walking uphill. Moreover, the hip joint has a wider ROM. It can accommodate more significant variations in joint angle, which may allow for more notable changes in the moment during uphill walking compared to the knee joint.

Many of this study's kinematic and kinetic results reflect previous research findings, but some aspects deviate from the existing consensus. The exact causes for any observed discrepancies cannot be determined within the scope of this study due to limitations discussed in Section 5.5. While measurement error is a possible factor, other variables, such as the treadmill setting and possible methodological differences must also be considered. Notably, Lay's[25, 27] and McIntosh's[20] research groups conducted the measurements on a walkway rather than a treadmill. This difference in the experiment environment could explain some of the observed deviations.

When comparing data from studies on a treadmill with those collected in the lab,

some studies have shown significant differences in hip and knee moments [48, 49, 50]. It highlights the potential impact of the measurement setting on joint moments, particularly under inclined conditions. Using a treadmill for walking could lead to changes in gait mechanics, including joint angles and moments, which may contribute to discrepancies compared to walkway-based experiments.

Additional data collection on both the treadmill and the lab ground would be valuable to investigate these uncertainties. Such a comparative study could provide information on the validity of the results of measurements on the treadmill. By systematically analyzing and comparing data from different study environments, one can better understand the possible effects of the treadmill setting on the observed joint angles and moments, thus improving the credibility and possibility of generalizing the results.

5.2 Muscular Implications and Contributions

The GM exhibits a force-length relationship in its sarcomeres, similar to other skeletal muscles. Consequently, there is an optimal FL at which the muscle operates most efficiently. Lichtwark and Wilson[35] have investigated the impact of walking strategies on muscle utilization. They furthermore state that "[...] efficient walking requires shorter muscle fascicles [...]"[35]. This observation suggests that the optimal FL may be shortened to enhance walking efficiency.

In the majority of the participants in this study, an increase in the range between minimum and maximum length was observed with increasing steepness, accompanied by a decrease in the maximum length itself. The mean peaks were significantly lower during 10° incline walking (Table 4.3). Lichtwark and Wilson[35] agree that the GM's optimal FL can range from 45 to 70 mm for level walking. Fascicle lengths of the conducted study range from 44.45 mm to 48.42 mm during level

walking, which is slightly shorter. Mean minimum values of 40.75 mm for the inclined walking and peak values of only 46.63 mm have been measured. Outcomes like this indicate that the body needs to make specific adjustments to maintain stability and efficiency during walking. Individuals may naturally adjust their gait and muscle activation patterns to accommodate the altered terrain as the incline angle increases.

The increase in the range between the minimum and maximum lengths of the muscle from 4.0 mm to 5.69 mm suggests that participants are likely to use a wider ROM of the gastrocnemius medialis to manage the incline. This increased variability in muscle length may reflect the need for greater flexibility and dynamic control to cope with the changing demands of the incline. The reduction in total muscle length could be explained due to the participants taking a more controlled and energy-efficient stride. Walking at an incline requires more effort due to the steepness and the body might respond by shortening the total muscle length to optimize energy expenditure. Lower mean peak values observed when walking on a 10° inclined surface could indicate that the participants use the gastrocnemius medialis muscle with less force than when walking on a flat surface. This could be due to the increased use of other muscles or the need for a more controlled and careful gait to avoid slipping or tripping on the sloping surface.

It should be emphasized that the ultrasound results from this study differ from the conclusions of previous research. Fukunaga et al.[18], Lichtwark et al.[35], and Lichtwark and Wilson[28] have reported considerably higher mean peak values of more than 54 mm in their respective studies. Notably, Lichtwark and Wilson even identified a significant decrease in peak values during 10° incline walking. However, it is worth highlighting that none of these previous studies involved a participant pool as extensive as the one utilized in this study (Lichtwark and Wilson: 6 participant; McIntosh et al.: 11 participant; Lay et al.: 9 participant;

Fukunaga et al.: 6 participants). This raises questions about the comparative significance of the results obtained in this study.

Furthermore, it is crucial to acknowledge that several other factors could contribute to the divergence between the current study's findings and those of previous research. Potential challenges and errors in ultrasound analysis must be addressed among these factors. A comprehensive discussion of these limitations and their potential impact on the accuracy and interpretation of the collected data will be presented in later sections and Section 5.5.

5.3 Correlations

Contrary to original expectations, significanct correlation was only found for three pairs of values. First, it was assumed that the initial angles of the knee and hip correlate with the initial angle of the ankle, as these three joints work as a chain in the leg.

However, this hypothesis is only supported in 10° inclined walking between *IAA* and *IKA*. While there appears to be a potential correlation in Figure 4.10a, it could not be detected statistically. These changes during walking on a 10° incline can have several explanations. At the 10° incline, the body may adopt a more extended posture to counteract the incline and maintain stability. This change in posture could lead to a positive correlation between the initial ankle and knee angles as both joints adjust together to help balance the body. During level walking, a more extensive day-by-day task, the joint and involved muscle adjustment might be more divided and less centered to the knee angle.

The opposite has been pointed out for *IAA* and the maximum hip extension moment. A clear correlation has been analyzed in level walking with a coefficient of $R = .526$. This outcome was not repeated when walking on a 10° slope. The

main goal during level walking might be to maintain an upright posture while establishing the most efficient gait strategy. The hip is intensely involved in keeping that posture and needs to coordinate the change of ankle angle. The body tends to lean forward when the ankle angle is higher during initial contact. To counteract this phenomenon, an increased moment must be applied for hip extension.
Furthermore, the hip moments might increase due to the body's biomechanical strategy for efficient forward movement. With 10° inclined walking, the focus is on a physiological change in gait, with maintaining stability and balance as the primary intention. As mentioned, the coordination of the ankle and hip joints becomes less important while the interaction between the ankle and the knee increases. That could also be interpreted as a factor why the *MHFM* does not change, further showing a decreasing tendency with the change of the walking condition. The main focus in this phase is on the knee and no longer on the hip joint.
An unexpected finding emerged from the correlation analysis between *IAA* and *USR*. Specifically, the pattern for level walking exhibits a positive but not significant change of value, as illustrated in Figure 4.9a. A different result was observed at an inclination of 10°, where the stretch range values decrease significantly as the initial ankle angle increases. With higher dorsiflexion on IC, the range of the length change in the gastrocnemius medialis decreases. It is worth mentioning that without the possible "outlier" at $USR \approx 6.5$ mm during level walking, this setup would also be correlated with almost the same correlation coefficient. This data point belongs to Participant 2, which, as one of the first participants, could contain measurement errors with higher probability. Placing the ultrasound probe was one of the most difficult tasks, as the experimenters lacked practice.
Walking on level ground is a routine activity requiring minimal cognitive effort and no significant physical adaptations. The gait mechanism appear to be straightforward in this case. In order not to stumble and fall, it is unnecessary to induce a

very high ankle angle during the initial foot contact. Nevertheless, the muscle is stretched more extensively directly when it is performed. A greater initial ankle angle leads to a wider ROM and muscle stretch, resulting in a positive correlation. On an incline, however, this simple gait mechanism is altered. More mechanisms will occur, and the interaction between the ankle and the muscles of the calf shift. The negative correlation indicates that as the ankle angle increases, the range of fascial stretching is smaller, reflecting the altered demands of walking uphill. For example, the ankle joint's stiffness and the calf muscles' tension may vary depending on walking conditions. While on level ground, the ankle joint may display greater flexibility, whereas when faced with an incline, the joint's stiffness might intensify. This would limit the ROM and lead to a negative correlation between the initial ankle angle and the muscle range. In addition, when navigating an incline, the requirement to lean forward from the hip, combined with the sloped terrain, might necessitate a consistently higher ankle angle throughout the entire gait cycle. This adaptation is likely to result in a quicker toe-off (as discussed in Section 5.1) directed more upward than forward, subsequently leading to a reduced range of fascicle length.

Furthermore, the observation could also be closely related to the concept of energy conservation. The body may strategically optimize muscle use patterns to minimize energy expenditure during uphill walking. In this way, the body could fine-tune its muscle use to ensure efficient energy use during the demanding task of walking up an incline by using more energy stored in the tendons, such as the Achilles tendon. Assuming that energy expenditure can be minimized by maintaining a near-isometric state, several conclusions can be drawn from the study's results. Hence, the primary goal would be to limit the fascicle length range addressed in order to facilitate the symbiotic relationship between muscle-tendon-unit in the calf and to reach the plateau region[41]. Accordingly, a practical recommendation to optimize energy

conservation during inclined walking, as shown in Figure 4.9b, could be to initiate the stance phase with a specific dorsiflexion angle to find the optimal *USR*, reducing the energy expenditure in the GM.

Based on the study, consideration could therefore be given to recommending a less dorsal gait for people suffering from hip pain. The significant increase in hip moments when walking on level ground, combined with the observed tendency when walking on an inclined surface, suggests that a reduction in the degree of initial foot flexion could reduce the demand on the hip joint. The hip joint is generally less involved in changing walking conditions as the moments show less expression change. That could be used as a further advantage by adjusting the initial dorsiflexion accordingly.

5.4 Variances Among Participants

As can be seen in Figure 4.4 and Table 4.2, specific individuals exhibit pronounced deviations from the overall trend. Participant 7, for example, shows the most marked change in the gastrocnemius length range and thus stands out. In contrast, Participant 5 shows a counterintuitive pattern where the fascicle stretch range decreases with increasing inclination. Figure 5.3 compares the progression of fascicle length and ankle, knee, and hip angle over one gait cycle for the two participants. Participant 1 was also included to provide an average result for comparison. Besides anatomical considerations that may influence these observations, different interactions between the muscles and joints to overcome the inclination may also be a factor that impacted the different outcomes.

The much higher *USR* value of Participant 7 poses challenges in interpretation within the context of the present findings. A slightly more extensive range of ankle angle is noted, but both knee and hip angle range and progression show no notice-

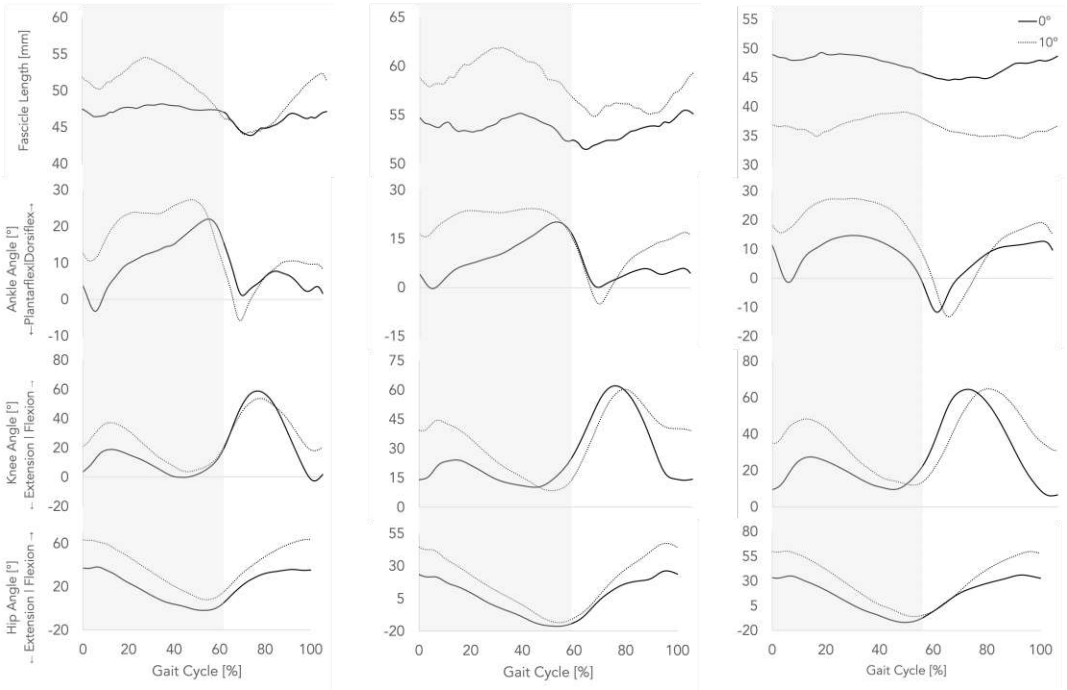

(a) Participant 7 (b) Participant 1 (c) Participant 5

Figure 5.3: Direct comparison of the fascicle length and angle (ankle, knee, and hip) progression for participants 7, 1, and 5. The gray shaded area indicates the stance phase, while the white area marks the swing phase.

able difference. It is worth noting that the initial knee angle and the minimum and maximum values are much smaller than in Participant 1. Nevertheless, comparable results can be seen for Participant 5, which does not have such a high *USR* value in the inclined state. Another aspect to consider regarding the knee is the narrower range of initial angles when comparing the two walking setups. Keeping the knee in a more neutral position upon initial contact potentially influences the engagement of lower limb muscles to compensate for stability and facilitate forward movement during the incline. This multi-layered interaction and the lack of clear explanations underline the complexity of biomechanical adaptations. It also shows that other factors, such as different muscle architectures or muscle recruitment strategies, must be taken into account.

In contrast to Participants 1 and 7, the absence of distinct dorsiflexion just prior to TO is conspicuous in Participant 5. This could contribute to a relatively limited ROM for the muscle. Additionally, Participant 5 exhibits a notably elevated plantar flexion value during TO, which may contribute to maintaining a stable fascicle length. Hence, an interesting question arises regarding the discrepancy between these observations and the results of the US. The transition from maximum dorsiflexion to plantarflexion is pronounced. Nevertheless, the US measurements do not reflect a correspondingly higher *USR* for the inclined state. This cannot be explained by comparing the knee or hip angles, of which the ranges are similar to the other two participants. This aspect could be examined more closely in future studies.

Another influential factor may be walking speed. Participant 5 chose the fastest speed at $1.39\frac{m}{s}$. Higher rate of motion could contribute to a shorter fascial length due to the increased muscle contraction required to generate the necessary force during the ascent. This increased contraction could potentially limit the amount of variation in fascicle length. Such a phenomenon could also explain why the FL values are significantly lower during the inclined walking condition. In addition, the GM could adapt to the altered biomechanics of uphill walking. This adaptation could consist of optimizing both force generation and joint stability. One plausible strategy is maintaining a relatively constant fascicle length range, thus ensuring efficient power transmission, which is particularly important during faster walking.

5.5 Limitations

Apart from the findings contributing to a better understanding of how our bodies adapt to walking on slopes and the factors influenced by the variation in foot position at initial contact, it is essential to acknowledge certain limitations in the

study. Discussing these limitations allows for future research to address thse issues effectively.

Throughout this chapter, challenges encountered in handling the US data were highlighted. Selecting a fascicle with consistent and clear visibility proved difficult during processing. Finding a suitable fascicle proved difficult in some trials, and adjusting the contrast did not result in significant improvements. Consequently, the extracted results may need further refinement in terms of precision and reliability. This could be due to the complicated handling of ultrasound images, which requires a higher level of expertise. Possible sources of error lie both in the use of the ultrasound probe, and in the subsequent data analysis. Despite adhering to the prescribed guidelines for attaching the ultrasound probe and comparing it with the optical feedback, there is an uncertainty factor due to the lack of experience, meaning that errors cannot be completely ruled out.

The guidance given by Farris and Lichtwark[65] when using the software was followed and even an alternative approach was attempted. However, running the algorithm multiple times occasionally led to different results, suggesting that the repetition rate may not have been sufficient to draw meaningful conclusions.

Ultrasound data offers a different perspective in movement biomechanics and represents a valuable opportunity to study muscle length changes. As Lay et al. have pointed out, this technique has yet to receive the attention it deserves. It holds great potential for future research, especially compared to kinematic and kinetic data[25].

Furthermore, including *USR_MAX* and *USR_MIN* in the study could bring exciting insight into how the muscle copes with an incline. Assuming that during inclined walking, *USR_MAX* demonstrates an increase compared to level walking, it may indicate a lengthening pattern within the muscle fascicle. Conversely, an increase in *USR_MIN* would suggest that the muscle maintains a shorter fascicle

length. Both results provide an intriguing insight into the dynamics of the calf muscle and its interaction with the joints of the lower body. Regardless, it is necessary to know more about the behavioral differences during statics and gait to include this. The observed higher static values compared to those during walking are valid and not due to processing errors, as assumed. The study of Hill's muscle model underlines the importance of considering the length of the fascicle and the entire length of the tendon connected to the muscle. This emphasizes that the properties of the muscle-tendon unit vary between the stance and movement phases. Therefore, integrating an analysis of tendon behavior into a future study could prove very beneficial.

The study is in agreement with prior studies but shows that for an understanding of inclined locomotion tasks, the consideration of the GM's FL is insufficient. A general perception exists that the muscle cannot be considered as a single component in the body. Combining the knowledge of a function unit of muscle and intrinsic tendon, the muscle-tendon unit (MTU) is helpful[28]. Studies by Lichtwark et al.[28, 35] showed a task- and velocity-dependent change in tendon and muscle length, which should be considered during the investigation. Thus, a constant walking velocity could yield better insights into the addressed system's behavior. Moreover, a meaningful analysis could include the GM and other muscles that influence lower body movement, such as the soleus and the vastae in the anterior thighs.

Furthermore, the sample size N raises notable discussion points. Specifically, certain samples in the study comprised only four data records, approaching the minimal threshold for statistical analyses. Even though statistics proved normally distribution for almost all sets, using a higher sample size is recommended. The inclusion of further cycles would show whether the unexpected results of some parameters are due to errors in the experimental design or represent the actual

behavior. Moreover, increasing the number of participants in the study can enhance its validity and increase the likelihood of identifying groups with similar behavior. The sensitivity analysis conducted for the correlation, utilizing a two-sided test with a type I error (α) of 0.05, indicated that, given the assumed power of 80% and the achieved sample size of 12 subjects, only large effects ($|R| \geq .6$, or respectively $|g| > 0.8$) can be reliably identified. Table 4.4 reflects this outcome, showing significance for coefficients near $|R| = .6$, while smaller effects lack statistical significance. Consequently, when dealing with effects smaller than .5, the design of this study falls below the standard power of 80%, leaving uncertainty regarding whether a non-significant result truly reflects the absence of the effect in reality or if the study is underpowered. Nevertheless, it is essential to emphasize that this study incorporated a larger participant cohort, in contrast to several other referenced studies (e.g., Lichtwark and Wilson: 6[28]; McIntosh et al.: 11[20]; Lay et al.: 9[25]; Fukunaga et al.: 6[18]).

CHAPTER 6

Outlook and Conclusion

The study reported in this thesis lays important groundwork for future studies. I now am able to refine methods and provide more robust data to the scientific community by addressing the limitations discussed above. In a new study, my primary objective would be identifying angle, moment, or muscle-tendon unit (MTU) change patterns. These findings would enable me to draw valuable insights for the design of walking aids, such as orthoses, prosthetics, or even footwear inserts, among other possibilities.

I propose enrolling a minimum of 82 subjects to achieve this goal. An a priori power analysis for correlation (two-tailed, type I error (α) = 0.05), assuming a power level of 80% and a medium effect size of $|R| = .3$ (or respectively $0.5 \leq |g| \leq 0.8$), indicates that a sample size of at least $N = 82$ is required to detect these medium effects. To make significant statements about small effects of $|R| \leq .1$ ($|g| < 0.5$), a collection of 779 samples would be necessary. However, conducting such a study is not feasible for a small institute.

I would also seek to ensure a diverse participant pool, with equal representation of men and women, to facilitate the investigation of potential gender inequalities.

Furthermore, this study will include inclines of 5°, 10°, 15°, and will extend to three conditions on a downhill slope (-5°, -10°, -15°). Especially during hiking, walking downhill can induce significant discomfort, particularly in the knee. This comprehensive approach aims to provide insights into whether different patterns of muscle and joint usage lead, for example, to fewer issues.

Furthermore, broadening the study scope to incorporate additional ultrasound measurements alongside the equipment utilized for kinematic and kinetic evaluation of lower limb joints from the preceding project would be beneficial. This comprehensive approach aims to examine the behavior of the gastrocnemius muscle and facilitate the assessment of Achilles tendon dynamics, significantly enhancing our understanding of the intricate interactions within the lower limb muscle-tendon unit across diverse walking conditions.

Gaining insights into the behavior of muscles and tendons during inclined locomotion holds practical significance for individuals involved in activities like hiking and treadmill training. To understand the interlinked processes in the body brings insights into possible incorrect loads in joints and muscles. As mentioned, during hiking, individuals often experience various pain locations and complaints by the end of the day. Some may report knee pain, while others may lament sore muscles. Also, slips and falls occur repeatedly, and their understanding is worth investigating. Besides specific initial preconditions, one reason could be the divergent loads of the lower body. With this knowledge, one can use supporting devices, such as orthoses, to enhance their walking patterns and prevent major injuries.

Despite the discussed limitations, my research addresses critical issues related to walking mechanics, pain, and injury prevention. It bridges the gap between biomechanics and ultrasound imaging and demonstrates the potential of combining these disciplines to understand muscle-tendon interactions better.

The study aimed to provide insights into the mechanics of walking on inclined

surfaces compared to level terrain. While the analysis couldn't confirm all initial hypotheses, significant insights were gained, indicating diverse adaptations of the gastrocnemius medialis among individuals and under various walking conditions. The study revealed complex relationships between muscles and joints, showing that defined values alter between walking conditions. Adjusting the foot's initial position also changes hip loading and maximum muscle shortening of the gastrocnemius medialis, with the latter being influenced by inclination.

The research project supports a better understanding of how bodies adapt to walking on slopes, providing insights into how the placement of the foot on initial contact can alter knee angle, hip moment, or fascicle stretch range. This knowledge is valuable for supporting athletes, developing fall prevention strategies, designing better walking spaces, and contributing to the development of prostheses that automatically adjust to changes in inclination.

In summary, despite facing challenges and limitations, the study represents an essential step toward understanding the complicated biomechanics of walking, particularly inclined locomotion. Acknowledging these limitations allows for future improvements and refinements to methods. The research's practical relevance, bridging biomechanics and ultrasound imaging, underscores its importance in solving problems related to gait mechanics, pain, and injury prevention. The perseverance and dedication to contributing to biomechanics aim to improve the lives of people dependent on a deeper understanding of walking mechanics for their well-being and mobility.

Bibliography

[1] L. R. Sheffler and J. Chae, "Hemiparetic gait," *Physical Medicine and Rehabilitation Clinics*, vol. 26, no. 4, pp. 611–623, 2015.

[2] D. Beckers and J. Deckers, *Ganganalyse und Gangschulung: therapeutische Strategien für die Praxis*, 1st ed. Heidelberg, Germany: Springer-Verlag, 1997.

[3] M. W. Whittle, *Gait analysis: an introduction*, 1st ed. Oxford, UK: Butterworth-Heinemann, 1991.

[4] ©2015 Vicon Motion Systems, "Capture and process a ROM trial," accessed April 24, 2022. [Online]. Available: https://documentation.vicon.com/nexus/v2.1/desktop/NexusWsN/Labeling/Capture_and_process_a_ROM_trial.htm

[5] K. A. Lamkin-Kennard and M. B. Popovic, *Biomechatronics; Chapter 4 - Sensors: Natural and Synthetic Sensors*, 1st ed. Academic press, 2019.

[6] D. A. Winter, *Biomechanics and Motor Control of Human Movement*, 4th ed. Hoboken, NJ, USA: Wiley, 2009.

[7] Qualisys AB, "System Setup #1," accessed April 24, 2022. [Online]. Available: https://www.qualisys.com/applications/human-biomechanics/markerless-motion-capture/

[8] © IMV Imaging 2023, "The A, B, M's – Ultrasound Modes Explained," accessed November 28, 2023. [Online]. Available: https://www.imv-imaging.com/en/2023/04/the-a-b-ms-ultrasound-modes-explained/

[9] M. Tilp, S. Steib, G. Schappacher-Tilp, and W. Herzog, "Changes in fascicle lengths and pennation angles do not contribute to residual force enhancement/depression in voluntary contractions," *Journal of Applied Biomechanics*, vol. 27, no. 1, pp. 64–73, 2011.

[10] P. Zellmann and S. Mayrhofer, "Entwicklung des Bergsports im Winter und im Sommer - Studie," Vienna, Autria, 2018, Conducted on behalf of: Institut für Freizeit- und Tourismusforschung.

[11] S. Galle, P. Malcolm, W. Derave, and D. De Clercq, "Uphill walking with a simple exoskeleton: Plantarflexion assistance leads to proximal adaptations," *Gait & Posture*, vol. 41, no. 1, pp. 246–251, 2015.

[12] R. C. Sheehan and J. S. Gottschall, "At similar angles, slope walking has a greater fall risk than stair walking," *Applied Ergonomics*, vol. 43, no. 3, pp. 473–478, 2012.

[13] B. R. Brandell, "Functional roles of the calf and vastus muscles in locomotion," *American Journal of Physical Medicine*, vol. 56, no. 2, pp. 59–74, 1977.

[14] D. Gordon, E. Robertson, and D. A. Winter, "Mechanical energy generation, absorption and transfer amongst segments during walking," *Journal of Biomechanics*, vol. 13, no. 10, pp. 845–854, 1980.

[15] F. E. Zajac and R. R. Neptune, "Biomechanics and muscle coordination of human walking Part I: Introduction to concepts, power transfer, dynamics and simulations," *Gait & Posture*, p. 18, 2002.

[16] G. S. Chleboun, A. B. Busic, K. K. Graham, and H. A. Stuckey, "Fascicle Length Change of the Human Tibialis Anterior and Vastus Lateralis During Walking," *The Journal of Orthopaedic and Sports Physical Therapy*, vol. 37, no. 7, pp. 372–379, 2007.

[17] S. Bohm, R. Marzilger, F. Mersmann, A. Santuz, and A. Arampatzis, "Operating length and velocity of human vastus lateralis muscle during walking and running," *Scientific Reports*, vol. 8, no. 1, p. 5066, 2018.

[18] T. Fukunaga, K. Kubo, Y. Kawakami, S. Fukashiro, H. Kanehisa, and C. N. Maganaris, "In vivo behaviour of human muscle tendon during walking," *Proceedings. Biological sciences*, vol. 268, no. 1464, pp. 229–233, 2001.

[19] M. Ishikawa, P. V. Komi, M. J. Grey, V. Lepola, and G.-P. Bruggemann, "Muscle-tendon interaction and elastic energy usage in human walking," *Journal of Applied Physiology (Bethesda, Md. : 1985)*, vol. 99, no. 2, pp. 603–608, 2005.

[20] A. S. McIntosh, K. T. Beatty, L. N. Dwan, and D. R. Vickers, "Gait dynamics on an inclined walkway," *Journal of Biomechanics*, vol. 39, no. 13, pp. 2491–2502, 2006.

[21] M. Haggerty, D. C. Dickin, J. Popp, and H. Wang, "The influence of incline walking on joint mechanics," *Gait & Posture*, vol. 39, no. 4, pp. 1017–1021, 2014.

[22] N. T. Pickle, A. M. Grabowski, A. G. Auyang, and A. K. Silverman, "The functional roles of muscles during sloped walking," *Journal of Biomechanics*, vol. 49, no. 14, pp. 3244–3251, 2016.

[23] K. Kawamura, A. Tokuhiro, and H. Takechi, "Gait analysis of slope walking: a study on step length, stride width, time factors and deviation in the center of pressure," *Acta medica Okayama*, vol. 45, no. 3, pp. 179–184, 1991.

[24] A. Leroux, J. Fung, and H. Barbeau, "Postural adaptation to walking on inclined surfaces: I. Normal strategies," *Gait & Posture*, vol. 15, no. 1, pp. 64–74, 2002.

[25] A. N. Lay, C. J. Hass, and R. J. Gregor, "The effects of sloped surfaces on locomotion: A kinematic and kinetic analysis," *Journal of Biomechanics*, vol. 39, no. 9, pp. 1621–1628, 2006.

[26] J. C. Wall, J. W. Nottrodt, and J. Charteris, "The effects of uphill and downhill walking on pelvic oscillations in the transverse plane," *Ergonomics*, vol. 24, no. 10, pp. 807–816, 1981.

[27] A. N. Lay, C. J. Hass, T. Richard Nichols, and R. J. Gregor, "The effects of sloped surfaces on locomotion: An electromyographic analysis," *Journal of Biomechanics*, vol. 40, no. 6, pp. 1276–1285, 2007.

[28] G. A. Lichtwark and A. M. Wilson, "Interactions between the human gastrocnemius muscle and the Achilles tendon during incline, level and decline locomotion," *The Journal of Experimental Biology*, vol. 209, no. 21, pp. 4379–4388, 2006.

[29] L. M. Silva and N. Stergiou, *Biomechanics and Gait Analysis; Chapter 7 - The basics of gait analysis*, 1st ed. Omaha, NE, USA: Academic Press, 2020.

[30] J. P. Holden, J. A. Orsini, K. L. Siegel, T. M. Kepple, L. H. Gerber, and S. J. Stanhope, "Surface movement errors in shank kinematics and knee kinetics during gait," *Gait & Posture*, vol. 5, no. 3, pp. 217–227, 1997.

[31] R. R. Neptune, S. A. Kautz, and F. E. Zajac, "Contributions of the individual ankle plantar flexors to support, forward progression and swing initiation during walking," *Journal of Biomechanics*, vol. 34, no. 11, pp. 1387–1398, 2001.

[32] J. Watkins, *Fundamental Biomechanics of Sport and Exercise*, 1st ed. New York, NY, USA: Routledge/Taylor & Francis Group, 2014.

[33] N. J. Cronin, C. P. Carty, R. S. Barrett, and G. Lichtwark, "Automatic tracking of medial gastrocnemius fascicle length during human locomotion," *Journal of Applied Physiology (Bethesda, Md. : 1985)*, vol. 111, no. 5, pp. 1491–1496, 2011.

[34] D. J. Farris and G. S. Sawicki, "Human medial gastrocnemius force-velocity behavior shifts with locomotion speed and gait," *Proceedings of the National Academy of Sciences of the United States of America*, vol. 109, no. 3, pp. 977–982, 2012.

[35] G. A. Lichtwark, K. Bougoulias, and A. M. Wilson, "Muscle fascicle and series elastic element length changes along the length of the human gastrocnemius during walking and running," *Journal of Biomechanics*, vol. 40, no. 1, pp. 157–164, 2007.

[36] G. de Monte, A. Arampatzis, C. Stogiannari, and K. Karamanidis, "In vivo motion transmission in the inactive gastrocnemius medialis muscle–tendon unit during ankle and knee joint rotation," *Journal of Electromyography and Kinesiology*, vol. 16, no. 5, pp. 413–422, 2006.

[37] A. Arampatzis, K. Karamanidis, S. Stafilidis, G. Morey-Klapsing, G. DeMonte, and G.-P. Brüggemann, "Effect of different ankle- and knee-joint positions

on gastrocnemius medialis fascicle length and EMG activity during isometric plantar flexion," *Journal of Biomechanics*, vol. 39, no. 10, pp. 1891–1902, 2006.

[38] R. Hager, T. Poulard, A. Nordez, S. Dorel, and G. Guilhem, "Influence of joint angle on muscle fascicle dynamics and rate of torque development during isometric explosive contractions," *Journal of Applied Physiology (Bethesda, Md. : 1985)*, vol. 129, no. 3, pp. 569–579, 2020.

[39] A. Leroux, J. Fung, and H. Barbeau, "Adaptation of the walking pattern to uphill walking in normal and spinal-cord injured subjects," *Experimental Brain Research*, vol. 126, no. 3, pp. 359–368, 1999.

[40] M. V. Narici, T. Binzoni, E. Hiltbrand, J. Fasel, F. Terrier, and P. Cerretelli, "In vivo human gastrocnemius architecture with changing joint angle at rest and during graded isometric contraction," *The Journal of Physiology*, vol. 496, no. 1, pp. 287–297, 1996.

[41] M. D. Binder, N. Hirokawa, and U. Windhorst, *Encyclopedia of Neuroscience; Chapter: Force-Length Relationship*, 1st ed. Berlin, Heidelberg: Springer-Verlag, 2009.

[42] W. Herzog, S. K. Abrahamse, and ter Keurs, Henk E. D. J., "Theoretical determination of force-length relations of intact human skeletal muscles using the cross-bridge model," *Pflugers Arch.*, vol. 416, no. 1-2, pp. 113–119, 1990.

[43] C. L. Vaughan, *Dynamics of Human Gait*, 2nd ed. Cape Town, South Africa: Kiboho Publishers, 1999.

[44] A. Falisse, S. Van Rossom, J. Gijsbers, F. Steenbrink, B. J. van Basten, I. Jonkers, A. J. van den Bogert, and F. De Groote, "Opensim versus human body model: a comparison study for the lower limbs during gait," *Journal of Applied Biomechanics*, vol. 34, no. 6, pp. 496–502, 2018.

[45] L. Ren, R. K. Jones, and D. Howard, "Whole body inverse dynamics over a complete gait cycle based only on measured kinematics," *Journal of Biomechanics*, vol. 41, no. 12, pp. 2750–2759, 2008.

[46] B. Rosenhahn, T. Brox, U. Kersting, A. Smith, J. Gurney, and R. Klette, "A system for marker-less motion capture," *Künstliche Intelligenz*, vol. 1, no. 2006, pp. 45–51, 2006.

[47] S. Papegaaij and F. Steenbrink, "Clinical Gait Analysis: Treadmill-based vs Overground," pp. 1–8, 2017, published White Paper by Motek Medical Amsterdam.

[48] P. O. Riley, G. Paolini, U. Della Croce, K. W. Paylo, and D. C. Kerrigan, "A kinematic and kinetic comparison of overground and treadmill walking in healthy subjects," *Gait & Posture*, vol. 26, no. 1, pp. 17–24, 2007.

[49] S. J. Lee and J. Hidler, "Biomechanics of overground vs. treadmill walking in healthy individuals," *Journal of Applied Physiology*, vol. 104, no. 3, pp. 747–755, 2008.

[50] J. R. Watt, J. R. Franz, K. Jackson, J. Dicharry, P. O. Riley, and D. C. Kerrigan, "A three-dimensional kinematic and kinetic comparison of overground and treadmill walking in healthy elderly subjects," *Clinical Biomechanics*, vol. 25, no. 5, pp. 444–449, 2010.

[51] ©Vicon Motion Systems Ltd UK, "A deeper understanding of human movement," pp. 1–18, 2020, Vicon Official Press Release.

[52] Y. Zhou and Y.-P. Zheng, *Sonomyography: Dynamic and Functional Assessment of Muscle Using Ultrasound Imaging*, 1st ed. Singapore: Springer Nature, 2021.

[53] M. V. Franchi, B. J. Raiteri, S. Longo, S. Sinha, M. V. Narici, and R. Csapo, "Muscle Architecture Assessment: Strengths, Shortcomings and New Frontiers of in Vivo Imaging Techniques," *Ultrasound in Medicine & Biology*, vol. 44, no. 12, pp. 2492–2504, 2018.

[54] R. L. Lieber and J. Fridén, "Functional and clinical significance of skeletal muscle architecture," *Muscle & Nerve: Official Journal of the American Association of Electrodiagnostic Medicine*, vol. 23, no. 11, pp. 1647–1666, 2000.

[55] G. A. Lichtwark and A. M. Wilson, "Optimal muscle fascicle length and tendon stiffness for maximising gastrocnemius efficiency during human walking and running," *Journal of Theoretical Biology*, vol. 252, no. 4, pp. 662–673, 2008.

[56] A. J. Blazevich, N. D. Gill, and S. Zhou, "Intra-and intermuscular variation in human quadriceps femoris architecture assessed in vivo," *Journal of Anatomy*, vol. 209, no. 3, pp. 289–310, 2006.

[57] DFG - Deutsche Forschungsgemeinschaft, "The structural and mechanical recovery of soft tissues define joint-level function after acute injury: The healing of Achilles tendon rupture as a model system," accessed November 29, 2023. [Online]. Available: https://gepris.dfg.de/gepris/projekt/429519978?language=en

[58] S. Franklin, M. J. Grey, N. Heneghan, L. Bowen, and F.-X. Li, "Barefoot vs common footwear: A systematic review of the kinematic, kinetic and muscle activity differences during walking," *Gait & Posture*, vol. 42, no. 3, pp. 230–239, 2015.

[59] G. Bergmann, H. Kniggendorf, F. Graichen, and A. Rohlmann, "Influence of shoes and heel strike on the loading of the hip joint," *Journal of Biomechanics*, vol. 28, no. 7, pp. 817–827, 1995.

[60] Motek Medical B.V., "D-Flow - Gait tutorials," 2023, accessed November 20, 2023. [Online]. Available: https://knowledge.motekmedical.com/wp-content/uploads/2019/05/D-Flow-Gait-tutorials-1-4.pdf

[61] © 1992-2021 TELEMED, "Ultrasound Beamformer ArtUs EXT-1H," accessed January 11, 2022. [Online]. Available: https://www.pcultrasound.com/research/research_iosignals/

[62] ——, "Ultrasound Transducer LF9-5N60-A3," accessed January 11, 2022. [Online]. Available: https://www.pcultrasound.com/products/products_artus/

[63] B. Bolsterlee, S. C. Gandevia, and R. D. Herbert, "Effect of transducer orientation on errors in ultrasound image-based measurements of human medial gastrocnemius muscle fascicle length and pennation," *PLoS One*, vol. 11, no. 6, p. e0157273, 2016.

[64] C. L. Brockett and G. J. Chapman, "Biomechanics of the ankle," *Orthopaedics and Trauma*, vol. 30, no. 3, pp. 232–238, 2016.

[65] D. J. Farris and G. A. Lichtwark, "UltraTrack: Software for semi-automated tracking of muscle fascicles in sequences of B-mode ultrasound images," *Computer Methods and Programs in Biomedicine*, vol. 128, pp. 111–118, 2016.

Appendices

II Measurement questionnaire for patients

III Extended marker placement sheet of the HBM lower body model

Patientenanfrage: DFG-ATR Project

Probandennummer: _____ Messungsnummer:_____

Datum: _____

Versuchspersonal: _____

Geburtsdatum: _____ Gewicht: _____ kg

Männlich/Weiblich/Divers: _____ Größe: _____ cm

Dominante Seite: Links Rechts

Sportliche Aktivität (Stunden pro Woche):_____

Schuhgröße _____

Distanz Kniespalte → Lateral Malleolus

Links: _____cm Rechts: _____cm

Unterschenkelumfang @ 1/3 Distanz oben (vom Kniespalte)

Links: _____cm Rechts: _____cm

Notizen:

_____

_____

_____

_____

_____

_____

_____

_____

_____

_____

_____

_____

Page **1** of **1**

GAIT Workflow Sheet

This worksheet provides an overview of the basic workflow to perform a GAIT session. A more extensive explanation can be found in the system manual. For further questions please contact Motek Medical clinical application support at clinical.applications@motekforcelink.com or call +31 (0)20 301 3020.

Marker placement

The table on the right shows the marker placement of all markers in the HBM lower body model. Pay special attention to the placement of the markers printed **Bold** (or green in picture below); these are used during initialization to define the biomechanical skeleton. Accurate placement of these markers is essential for accurate results.
*These markers are optional. If used, they may be removed after model initialization.
** These markers are optional and only need to be used if trunk kinematics are desired.

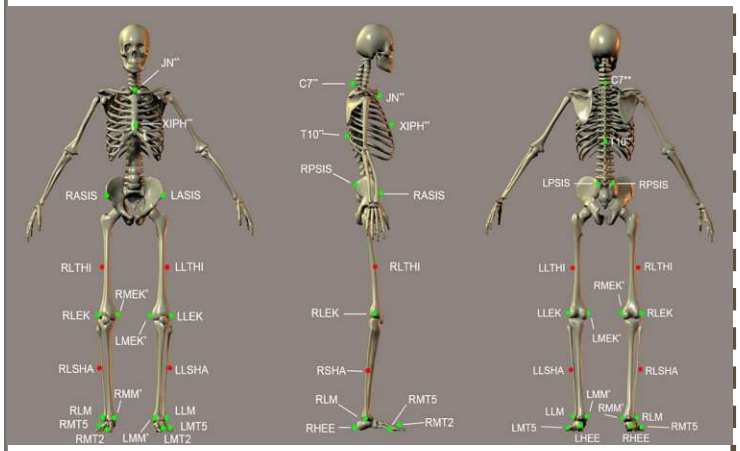

Motek
a DIH brand

No.	Marker	Position	Placement remarks
1	**C7****	**C7**	**On the 7th cervical vertebra**
2	**T10****	**T10**	**On the 10th thoracic vertebra**
3	**XIPH****	**Xiphoid process**	**Xiphoid process of the sternum**
4	**JN****	**Jugular notch**	**On the jugular notch of the sternum**
5	**LASIS**	**Pelvic bone left front**	**Left anterior superior iliac spine**
6	**RASIS**	**Pelvic bone right front**	**Right anterior superior iliac spine**
7	**LPSIS**	**Pelvic bone left back**	**Right posterior superior iliac spine**
8	**RPSIS**	**Pelvic bone right back**	**Right posterior superior iliac spine**
9	LLTHI	Left thigh, lateral	1/2 on the line between the left greater trochanter and LLEK
10	**LLEK**	**Left lateral epicondyle of the knee**	**On the lateral side of the joint axis**
11	**LMEK***	**Left medial epicondyle of the knee**	**On the medial side of the joint axis.**
12	LLSHA	Left shank, lateral	1/2 on the line between LLEK and LLM
13	**LLM**	**Left lateral malleolus of the ankle**	**The center of the left lateral malleolus**
14	**LMM***	**Left medial malleolus of the ankle**	**Most pronounced part of the left medial malleolus**
15	**LHEE**	**Left heel**	**Center of the heel at the same height as LMT2**
16	**LMT2**	**Left 2nd meta tarsal**	**Caput of the 2nd meta tarsal bone, on joint line midfoot/toes**
17	**LMT5**	**Left 5th meta tarsal**	**Caput of the 5th meta tarsal bone, on joint line midfoot/toes**
18	RLTHI	Right thigh, lateral	1/2 on the line between the right greater trochanter and RLEK
19	**RLEK**	**Right lateral epicondyle of the knee**	**On the lateral side of the joint axis**
20	**RMEK***	**Right medial epicondyle of the knee**	**On the medial side of the joint axis.**
21	RLSHA	Right shank, lateral	1/2 on the line between RLEK and RLM
22	**RLM**	**Right lateral malleolus of the ankle**	**The center of the right lateral malleolus**
23	**RMM***	**Right medial malleolus of the ankle**	**Most pronounced part of the right medial malleolus**
24	**RHEE**	**Right heel**	**Center of the heel at the same height as RMT2**
25	**RMT2**	**Right 2nd meta tarsal**	**Caput of the 2nd meta tarsal bone, on joint line midfoot/toes**
26	**RMT5**	**Right 5th meta tarsal**	**Caput of the 5th meta tarsal bone, on joint line midfoot/toes**